GaAs (semiconductor)

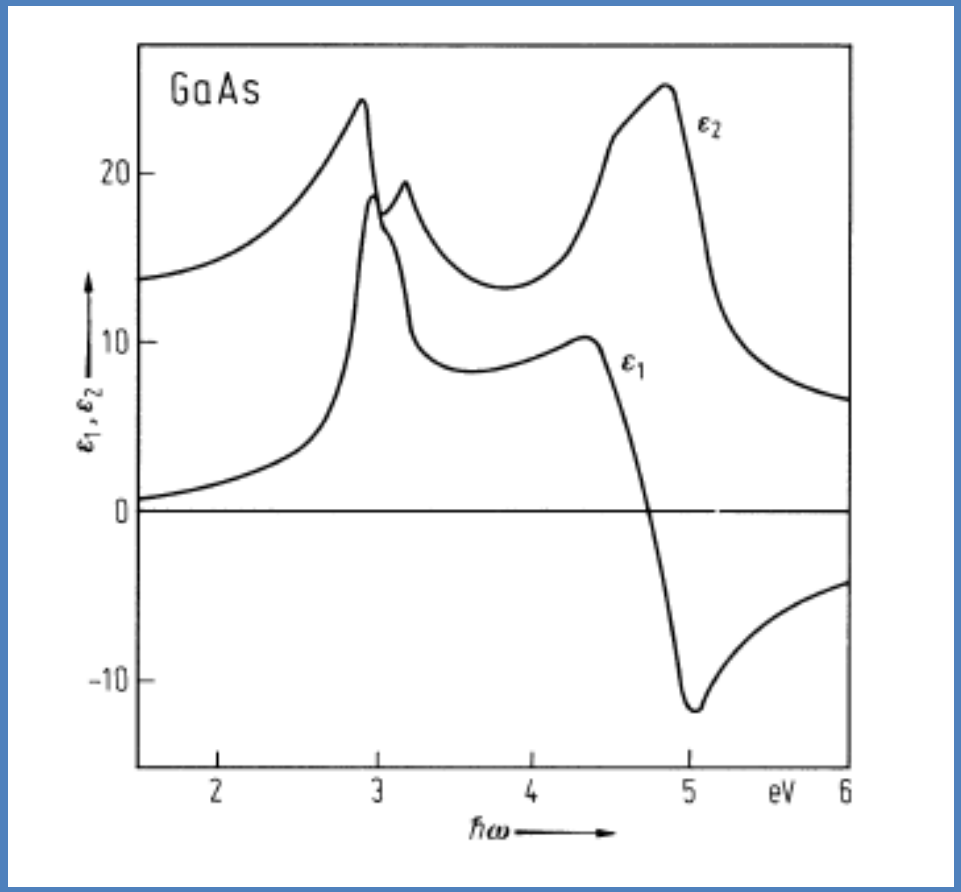

interband transitions

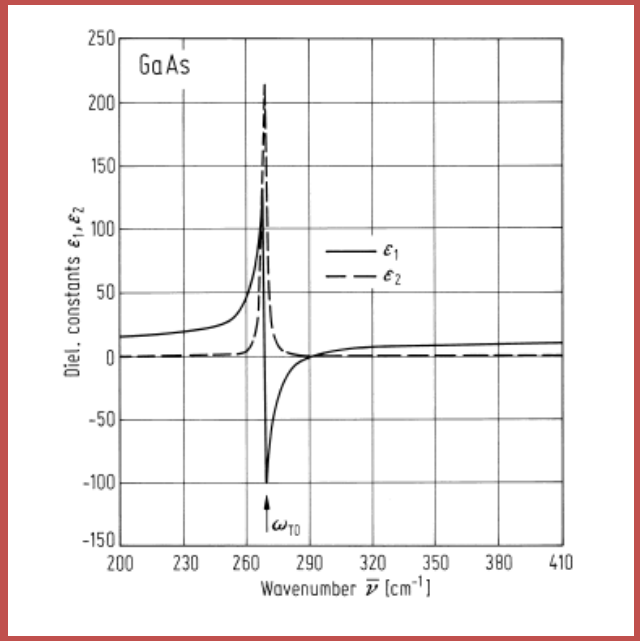

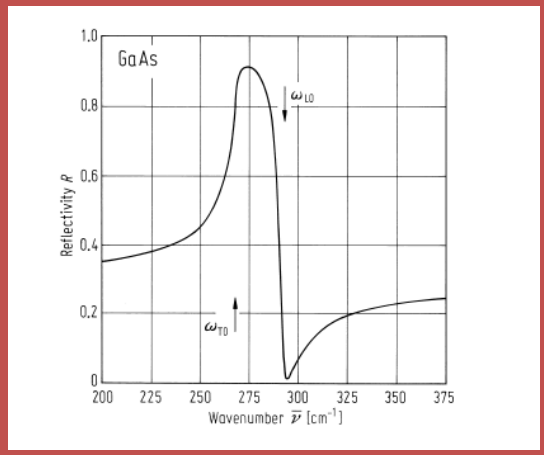

phonons

EXCITONS

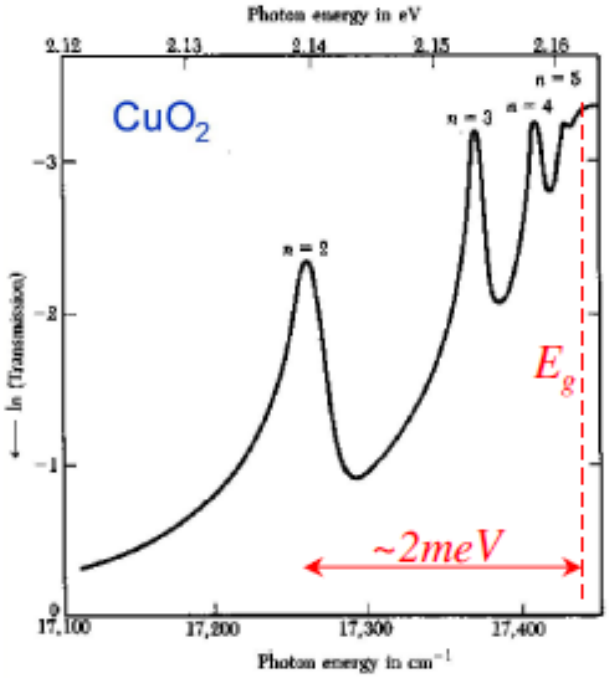
Photon energy in eV
2.12
2.13
2.14
2.15
2.16
CuO_2
n = 2
n = 3
n = 4
n = 5
E_g
~2meV
ln (Transmission)
17,100
17,200
17,300
17,400
Photon energy in cm^{-1}

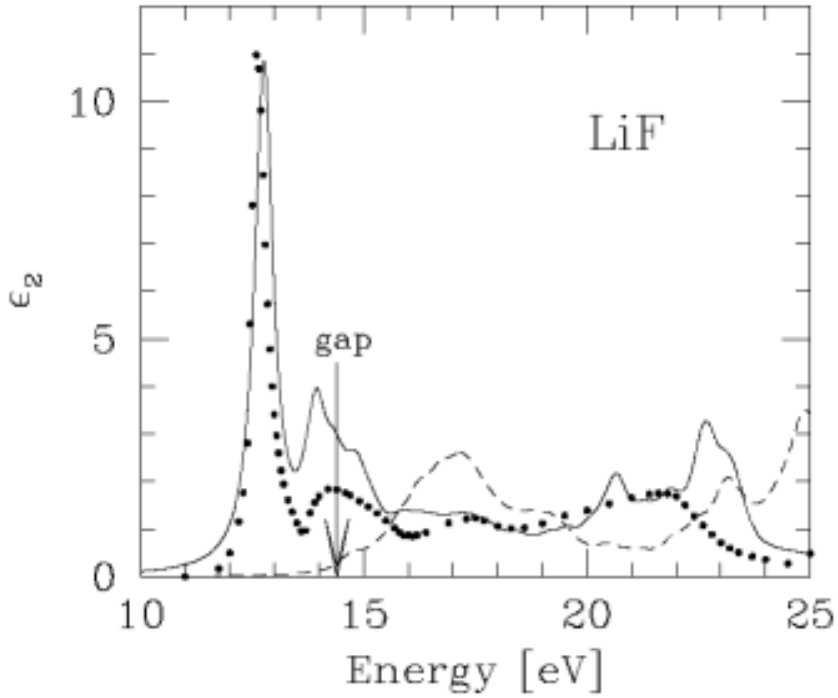
LiF
ϵ_2
gap
10
5
0
10
15
20
25
Energy [eV]

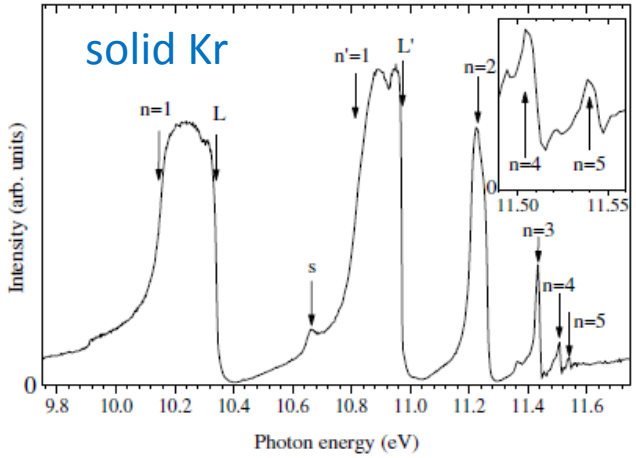
solid Kr
n=1
L
n'=1
L'
n=2
n=3
n=4
n=5
s
Intensity (arb. units)
0
9.8
10.0
10.2
10.4
10.6
10.8
11.0
11.2
11.4
11.6
Photon energy (eV)
11.50
11.55

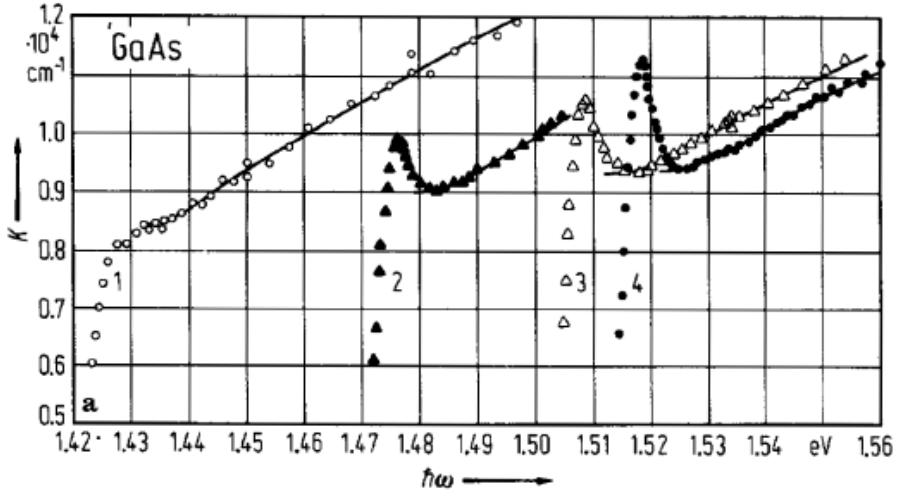
GaAs
10^4 cm^{-1}
K
1.2
1.0
0.9
0.8
0.7
0.6
0.5
a
1
2
3
4
1.42
1.43
1.44
1.45
1.46
1.47
1.48
1.49
1.50
1.51
1.52
1.53
1.54
eV
1.56
$\hbar\omega$

METALS AND DOPED SEMICONDUCTORS

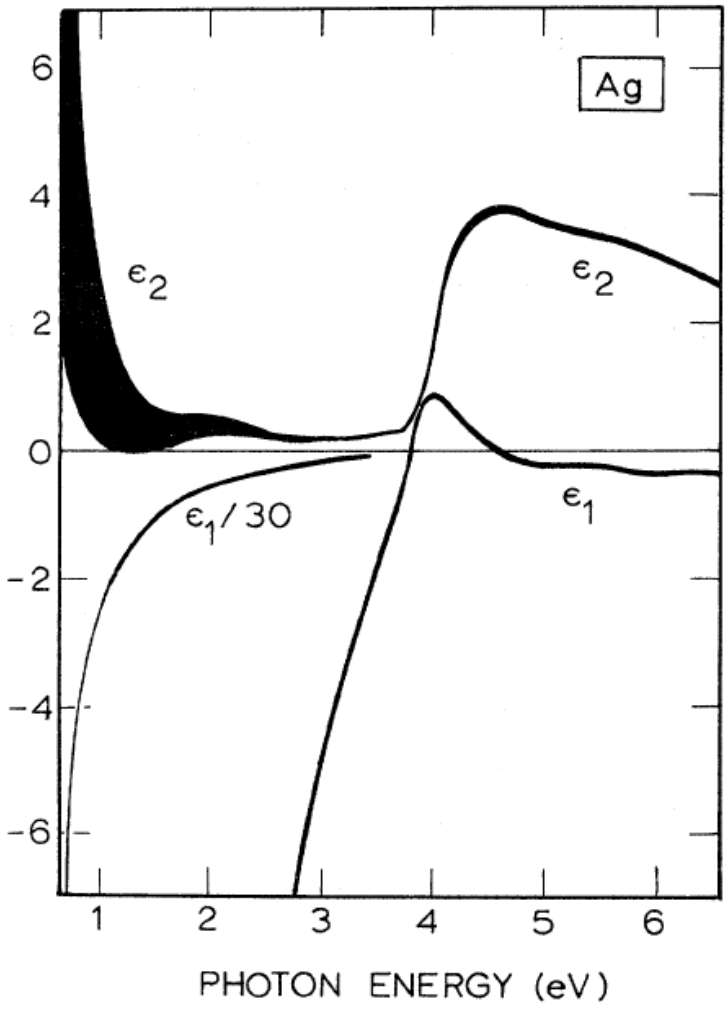

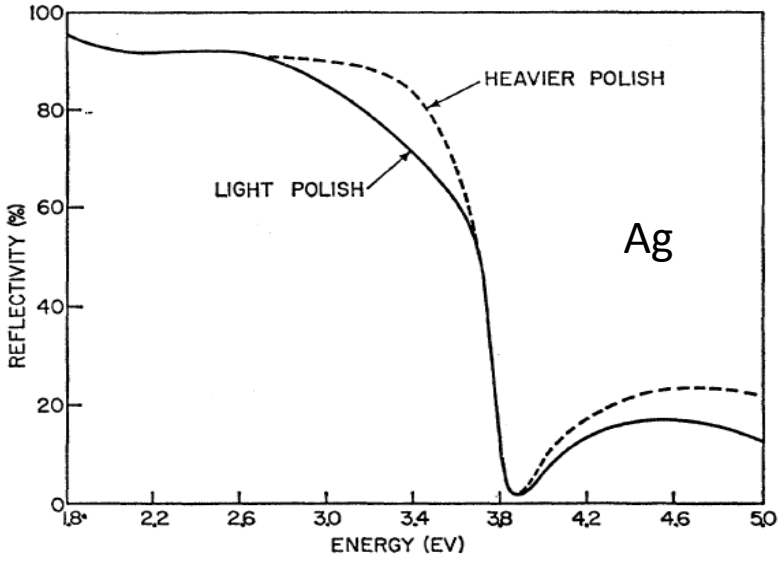

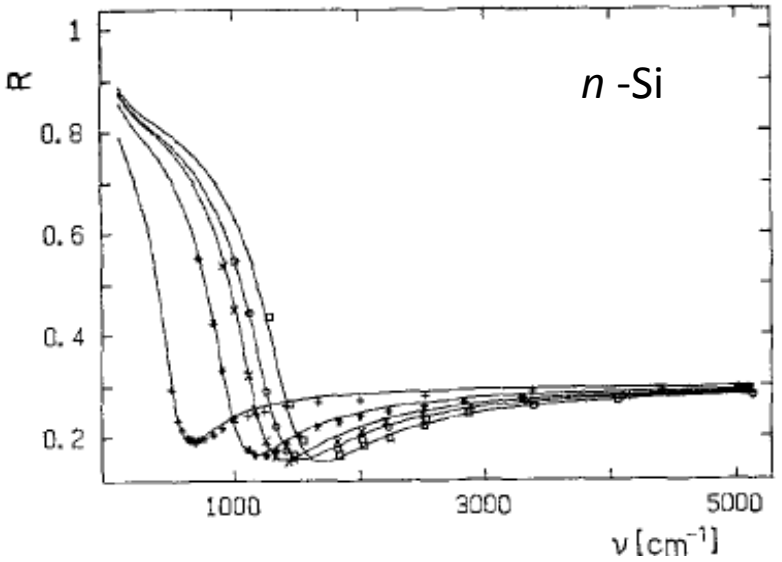

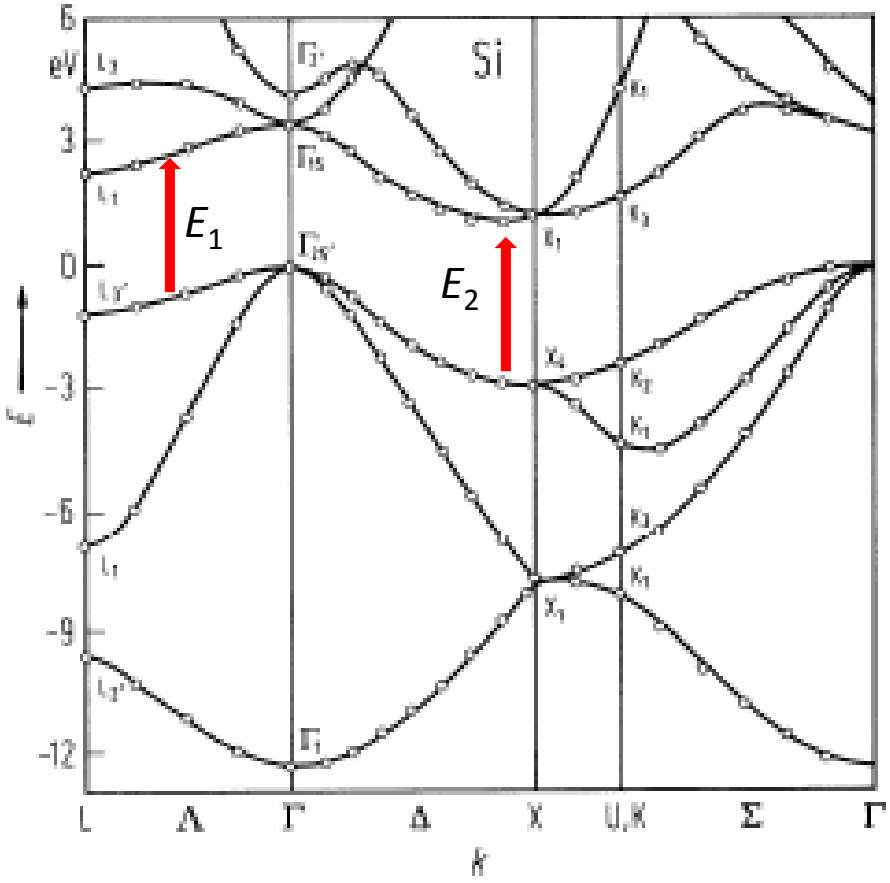

3D M_1-type critical point

near parallel bands:
2D M_0-type critical point

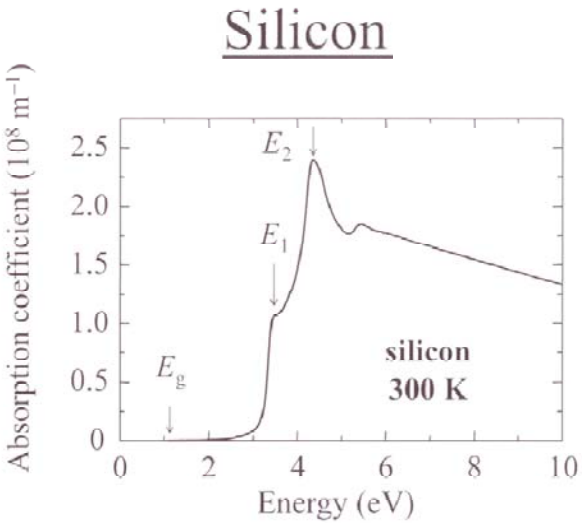

- Indirect band gap at 1.1 eV
- **Critical** points at E_1 (3.2 eV) and E_2 (4.3 eV)

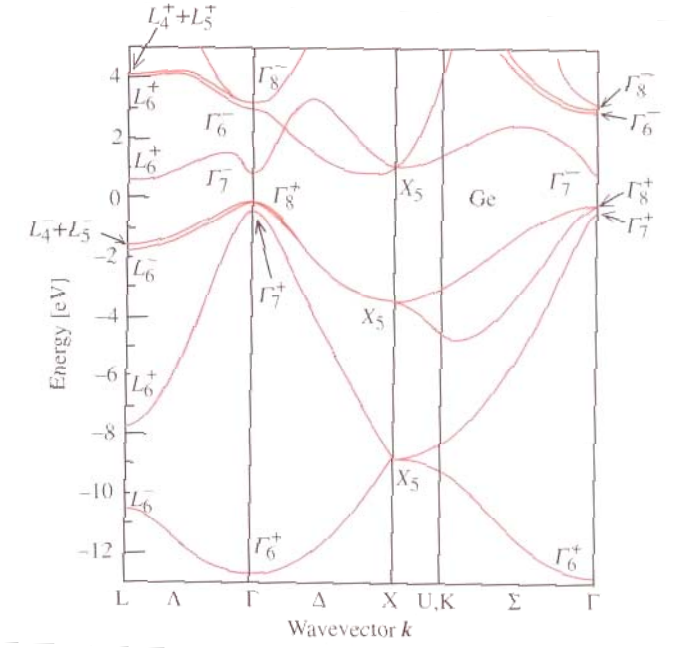
Energy [eV]
Wavevector k
L Λ Γ Δ X U,K Σ Γ
Ge

Ge

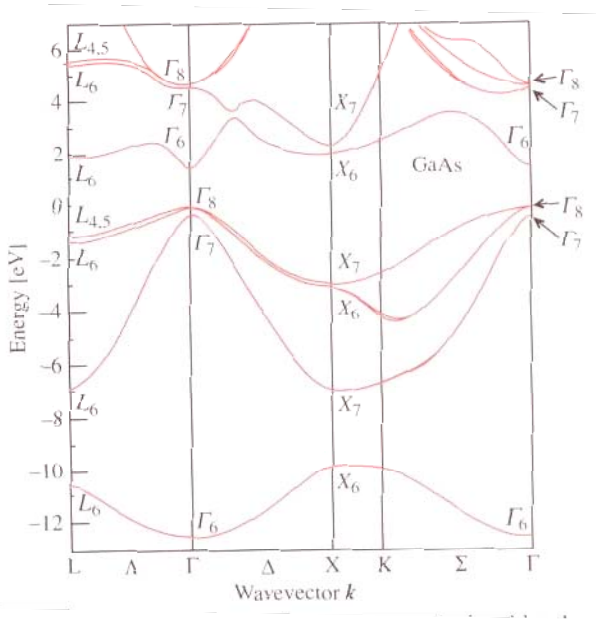
Energy [eV]
Wavevector k
L Λ Γ Δ X K Σ Γ
GaAs

GaAs

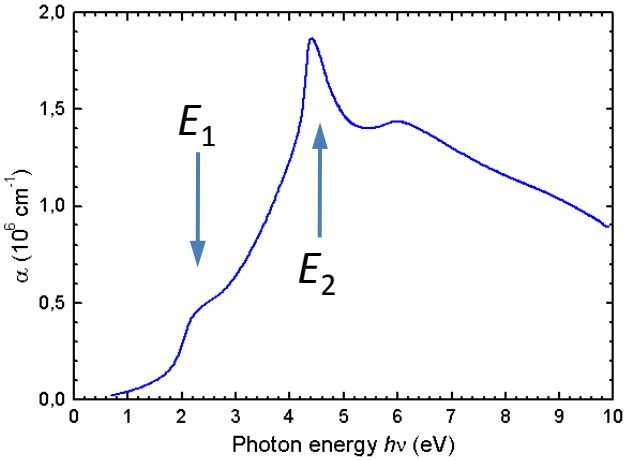
α (10^6 cm^-1)
Photon energy hν (eV)
E1
E2

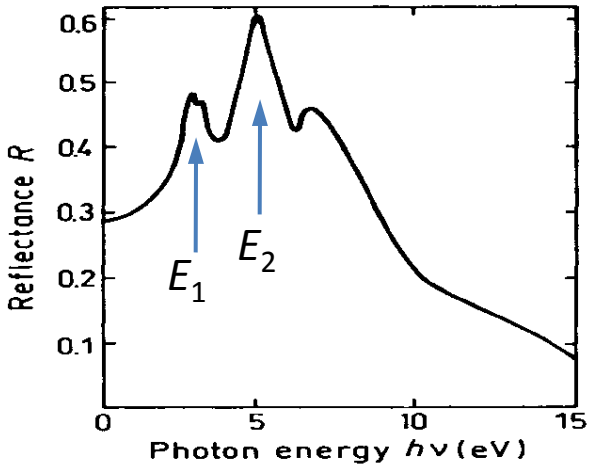
Reflectance R
Photon energy hν (eV)
E1
E2

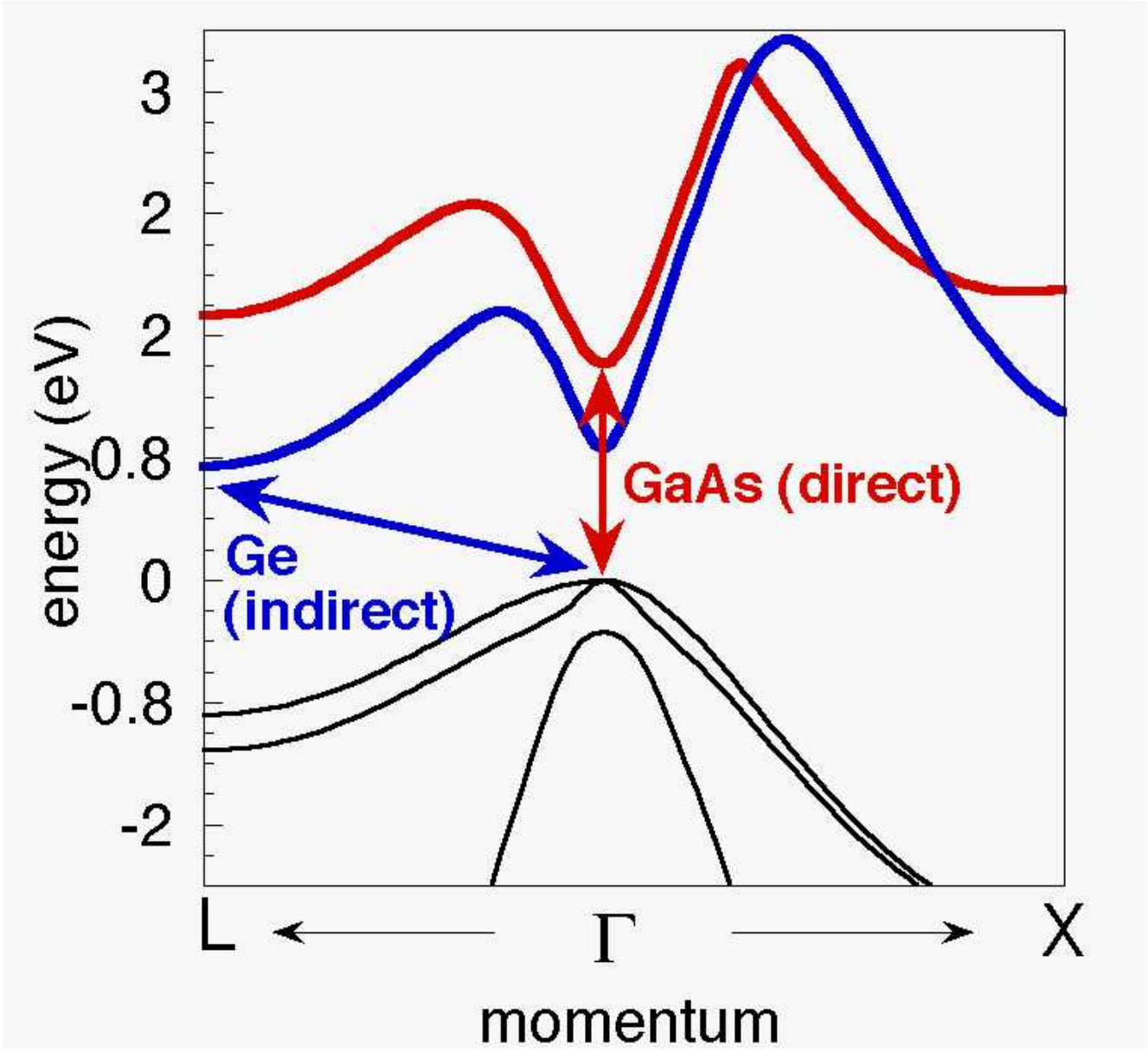
3
2
2
0.8
0
-0.8
-2
energy (eV)
GaAs (direct)
Ge
(indirect)
L
Γ
X
momentum

3D M_0-type critical point
(weak excitonic effects)

InAs band edge absorption

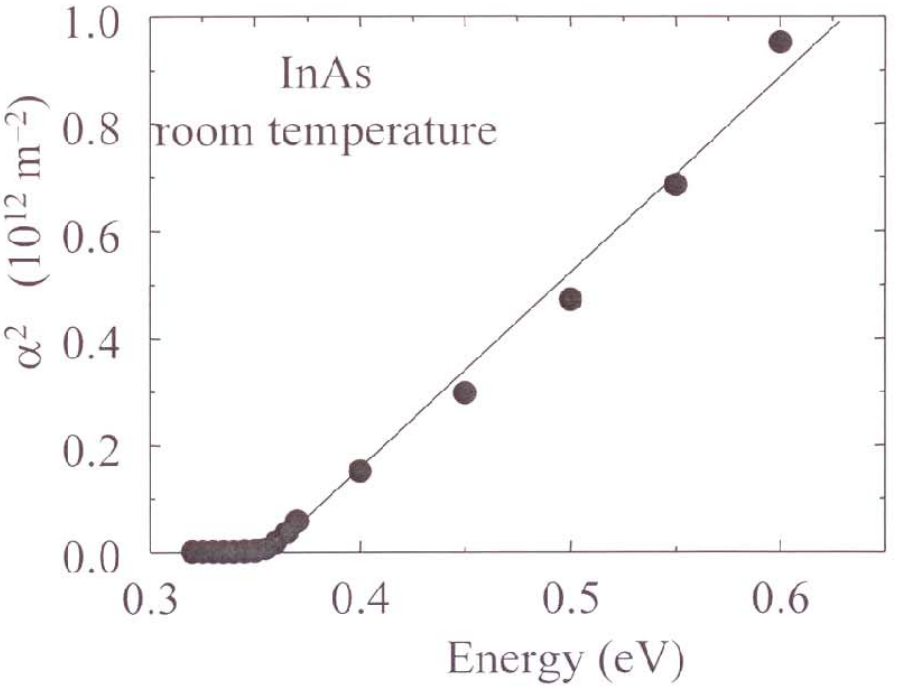

InAs is a direct gap III–V semiconductor with $E_g = 0.35$ eV

$\hbar\omega < E_g$: $\alpha = 0$

$\hbar\omega > E_g$:

$\alpha \propto (\hbar\omega - E_g)^{1/2}$

SPIN-ORBIT COUPLING

conduction band: $\begin{cases} \left|1\uparrow\right\rangle \equiv \left|+1/2\right\rangle \\ \left|1\downarrow\right\rangle \equiv \left|-1/2\right\rangle \end{cases}$

'heavy'-hole: $\begin{cases} \frac{1}{\sqrt{2}}\left|(X+iY)\uparrow\right\rangle & \left|J=3/2\,;m_J=+3/2\right\rangle \\ \frac{1}{\sqrt{2}}\left|(X-iY)\downarrow\right\rangle & \left|J=3/2\,;m_J=-3/2\right\rangle \end{cases}$

'light'-hole: $\begin{cases} \frac{1}{\sqrt{6}}\left|2Z\downarrow-(X-iY)\uparrow\right\rangle & \left|J=3/2\,;m_J=-1/2\right\rangle \\ \frac{1}{\sqrt{6}}\left|2Z\uparrow+(X+iY)\downarrow\right\rangle & \left|J=3/2\,;m_J=+1/2\right\rangle \end{cases}$

'split-off'-hole: $\begin{cases} \frac{1}{\sqrt{3}}\left|Z\uparrow-(X+iY)\downarrow\right\rangle & \left|J=1/2\,;m_J=+1/2\right\rangle \\ \frac{1}{\sqrt{3}}\left|Z\downarrow+(X-iY)\uparrow\right\rangle & \left|J=1/2\,;m_J=-1/2\right\rangle \end{cases}$

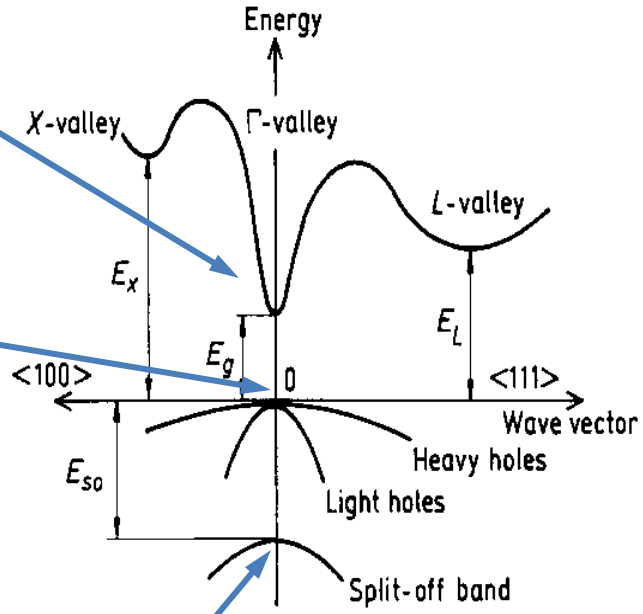

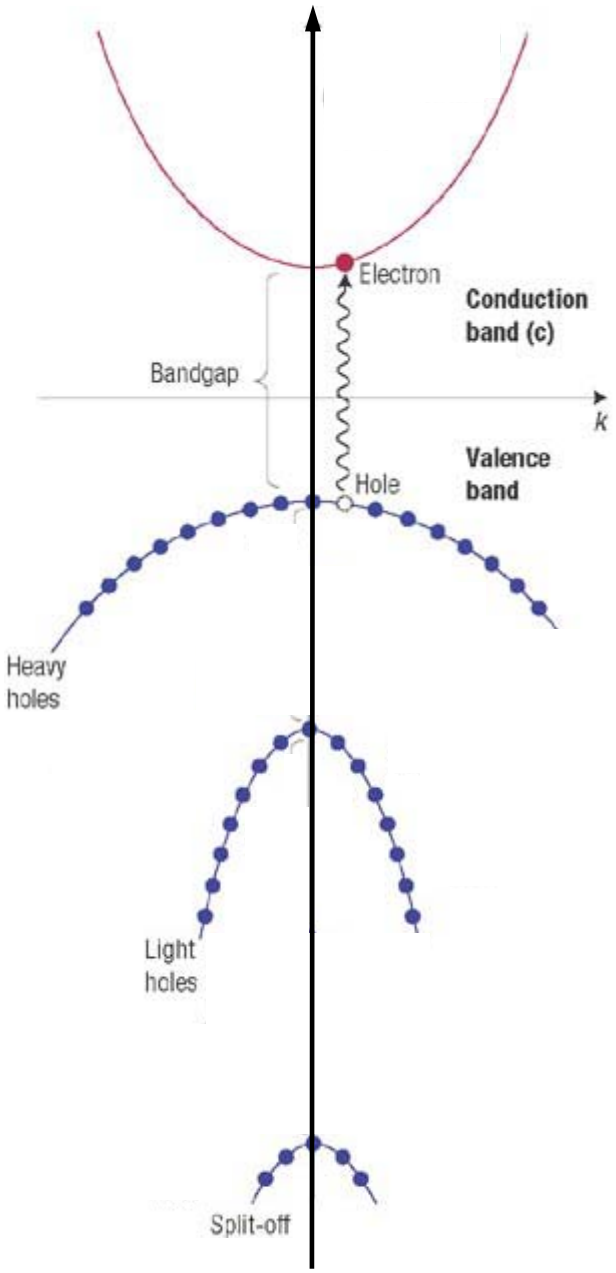

SPIN-ORBIT COUPLING

+

STRESS

(or quantum confinement)

SPIN-ORBIT COUPLING
+
UNIAXIAL [001] STRESS
(or quantum confinement)
+
EXTERNAL MAGNETIC FIELD

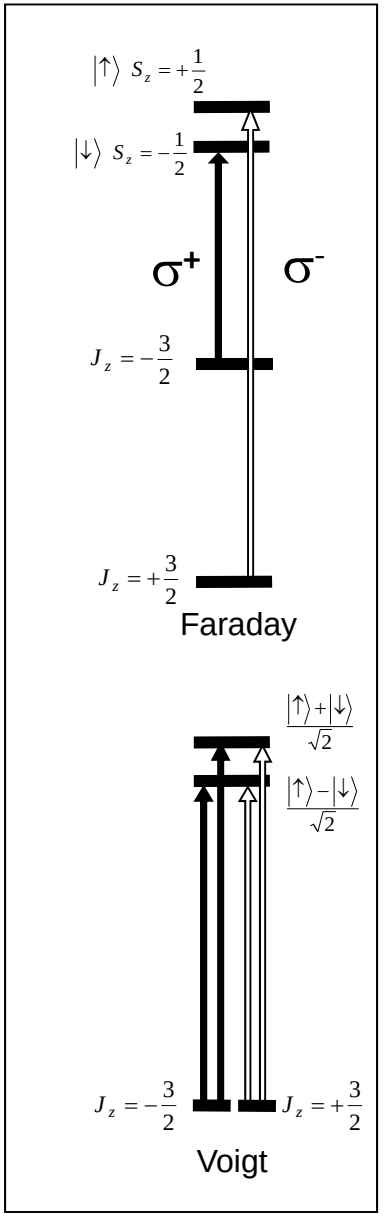

NOTES:
only heavy-hole states are shown for the valence band
$\sigma^{+/-}$ denote circular polarization

Faraday: **B** parallel to [001]
Voigt: **B** perpendicular to [001]

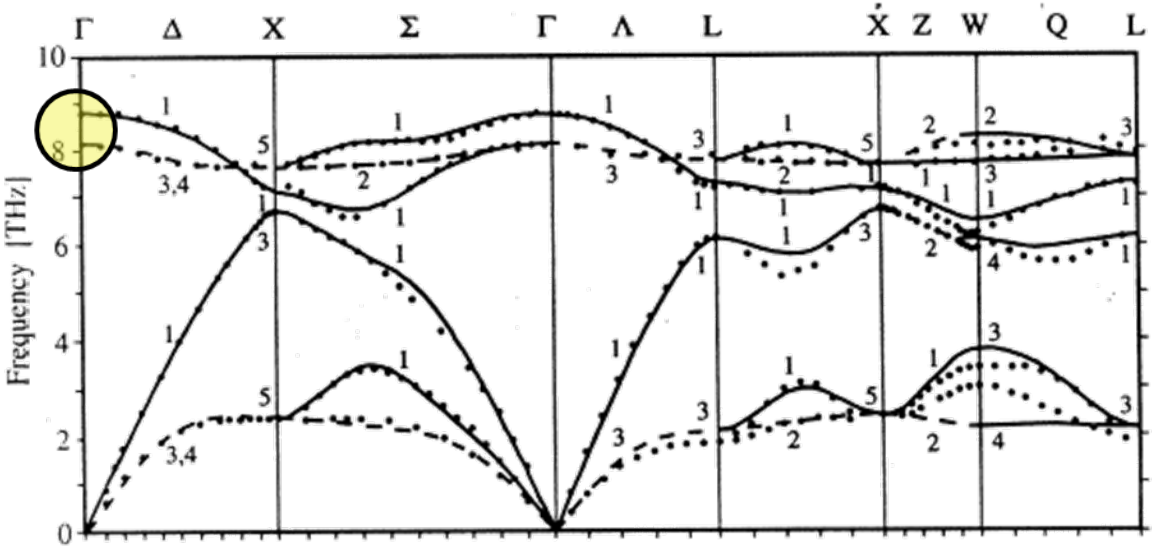

GaAs

Reflectivity

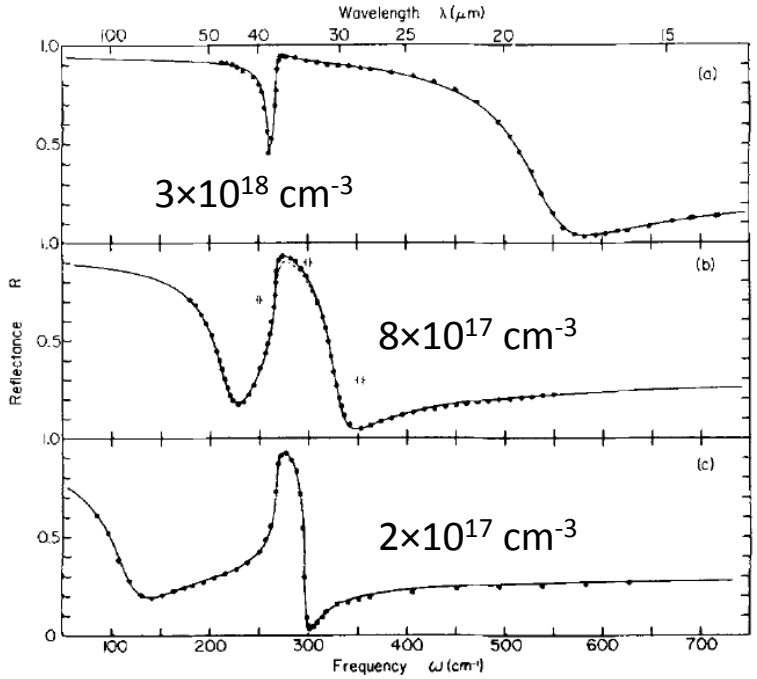

Two-Phonon Absorption

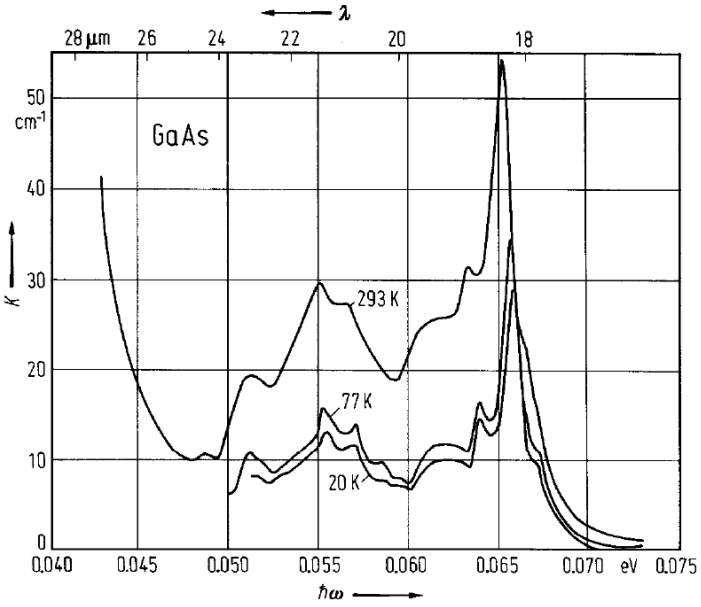

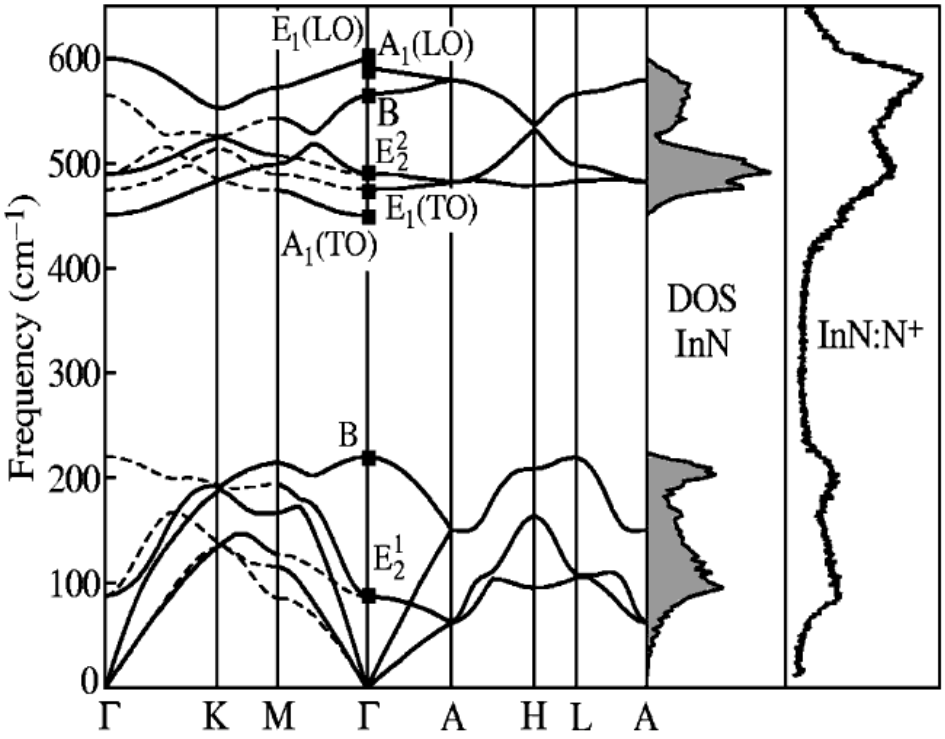

InN (wurtzite)

heavily doped

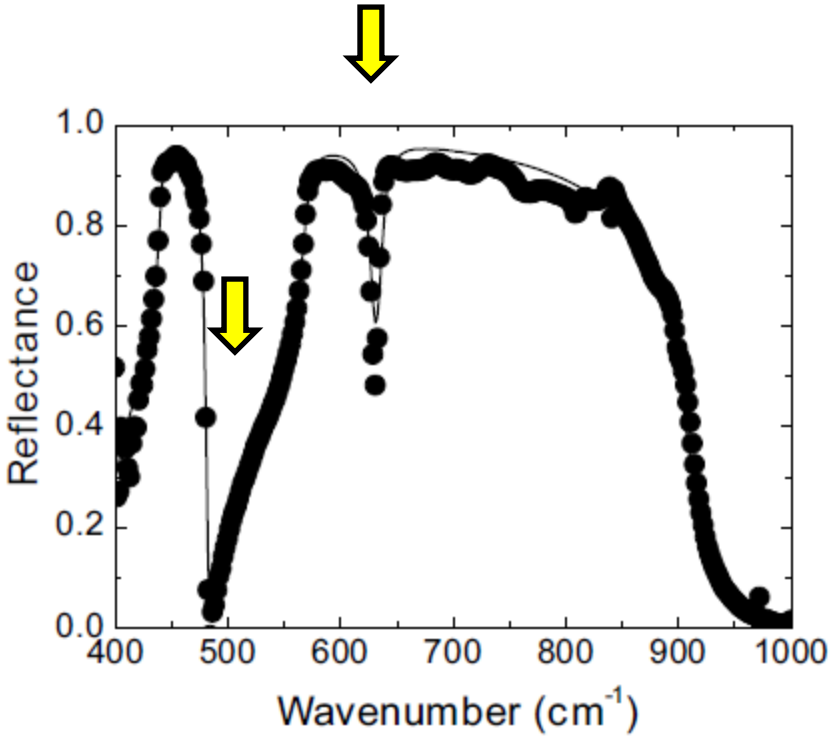

PbS (rock salt)

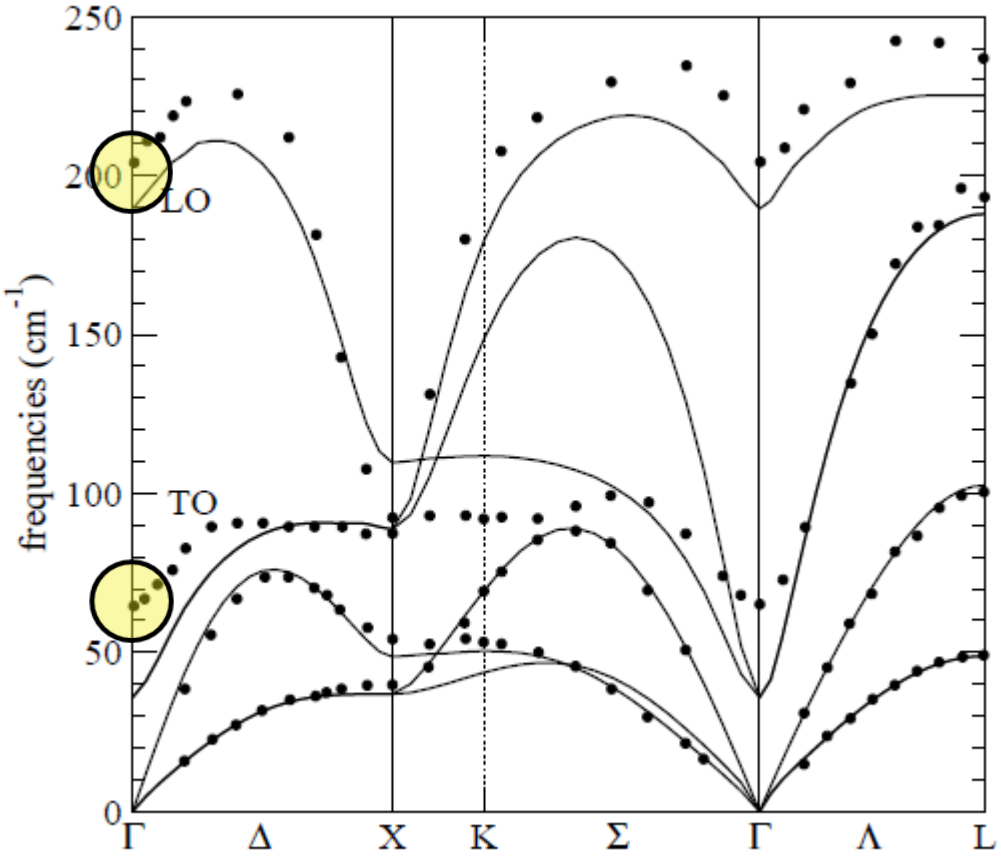

huge TO-LO splitting

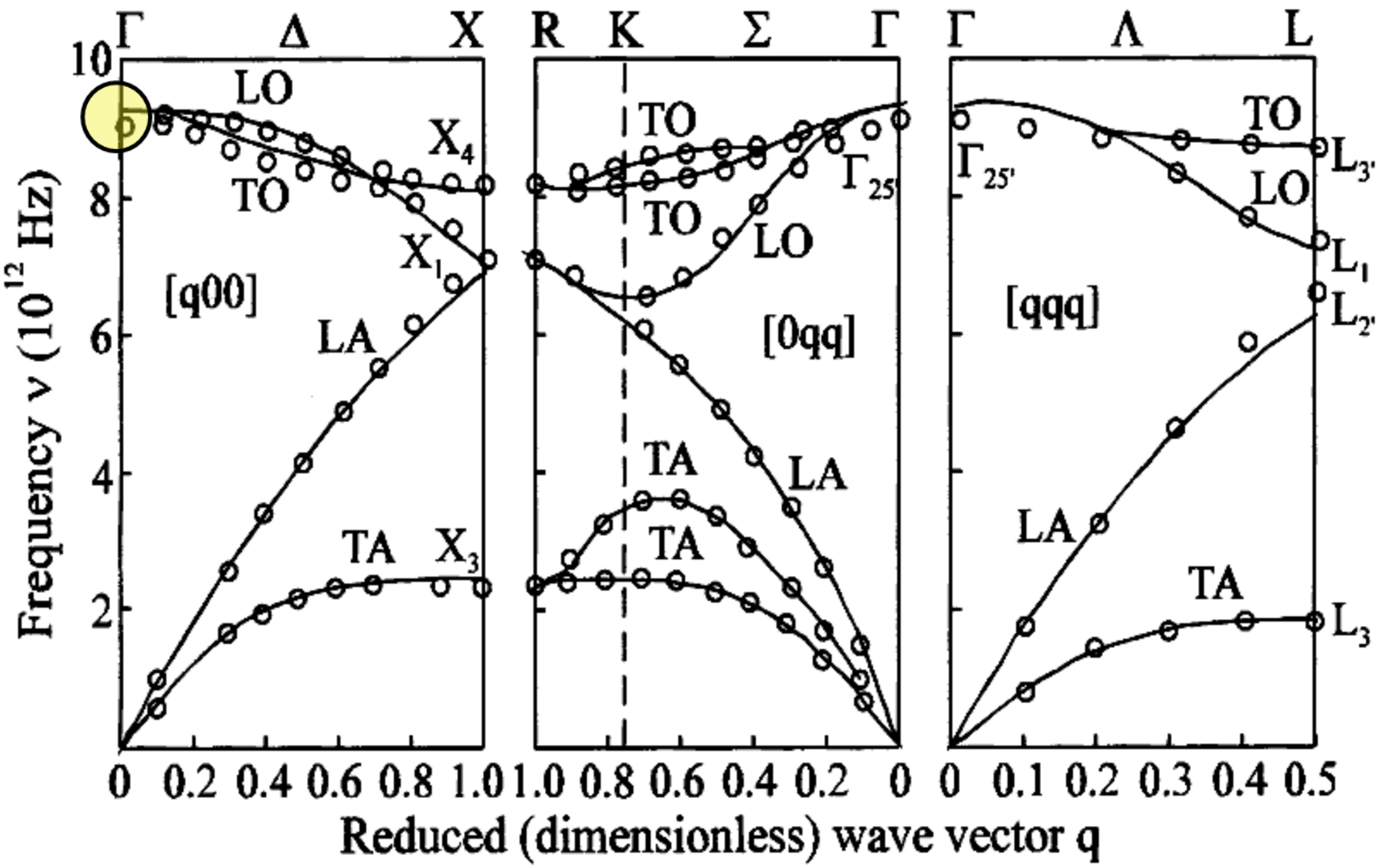

Germanium (IR inactive)

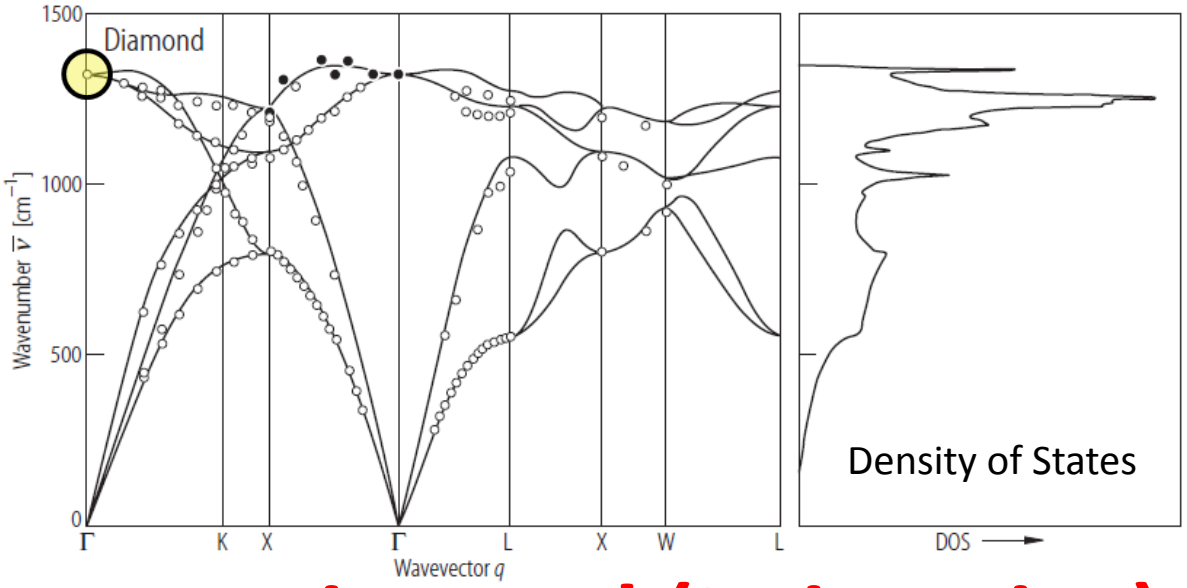

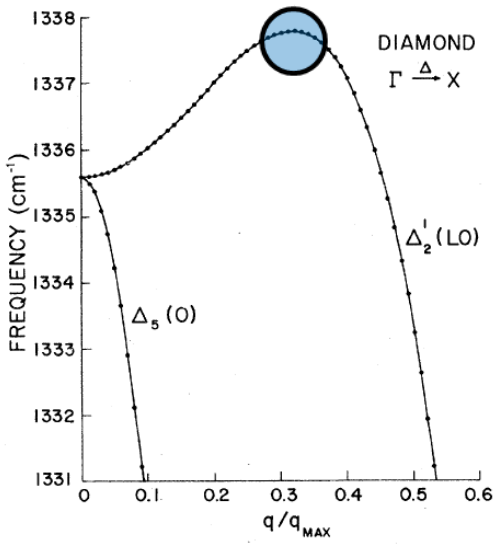

Diamond (IR inactive)

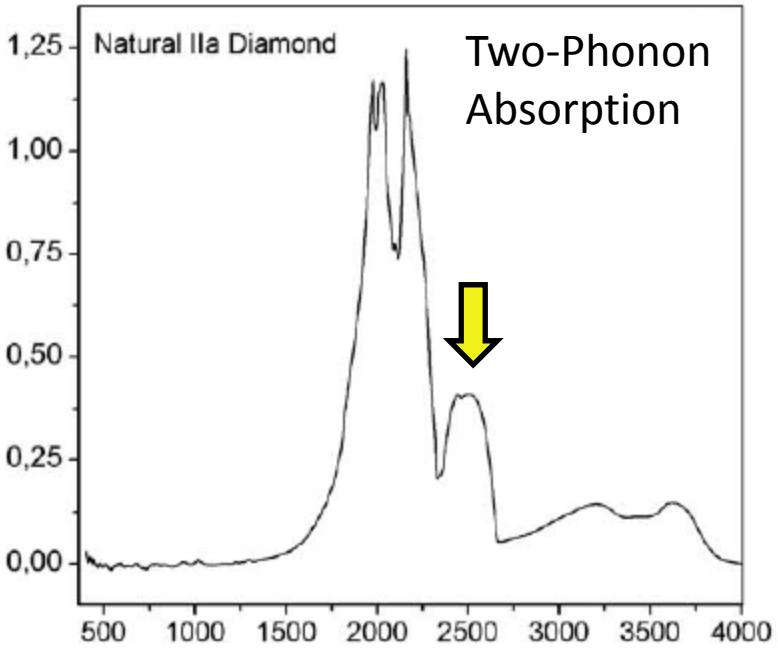

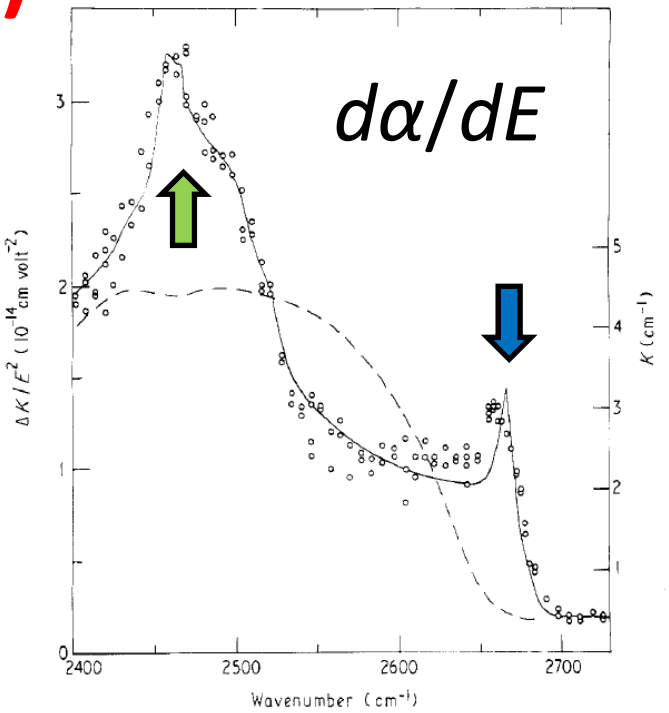

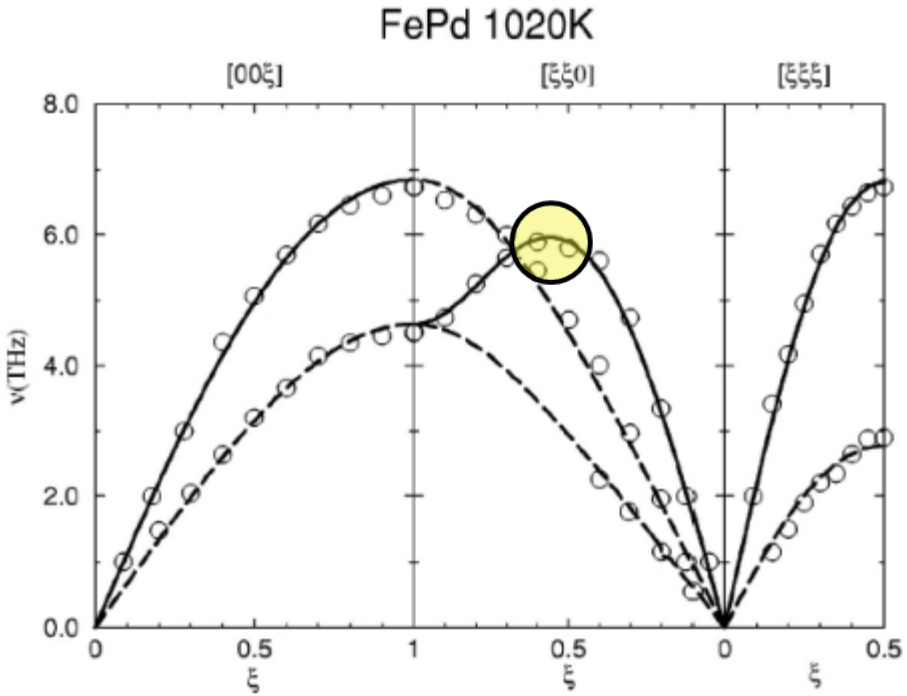

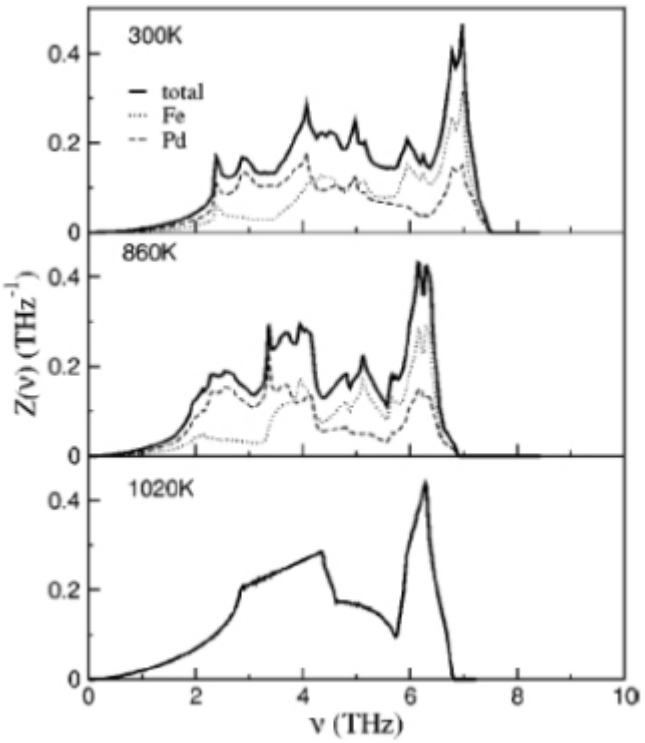

density of states

TaS_2: Kohn anomaly ($2k_F$)

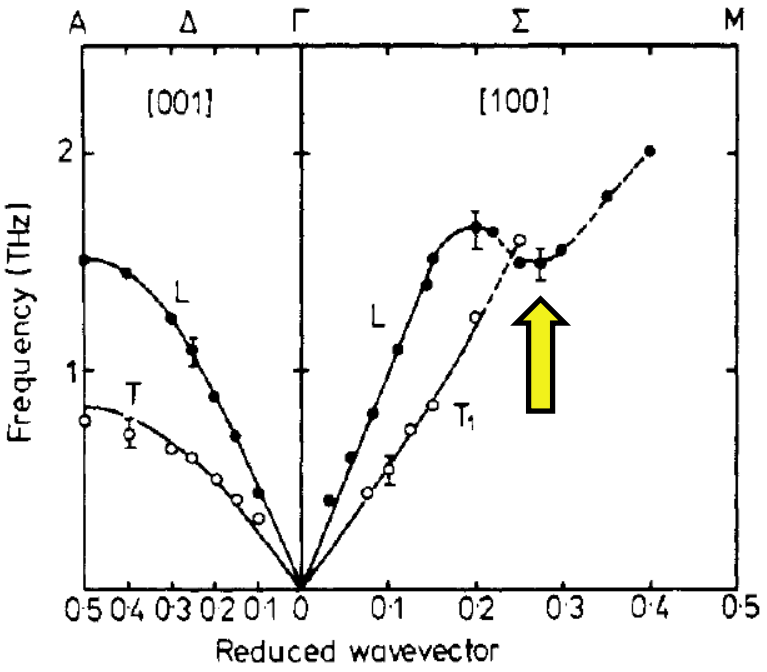

metals

bcc Vanadium:
Kohn anomaly ($2k_F$)

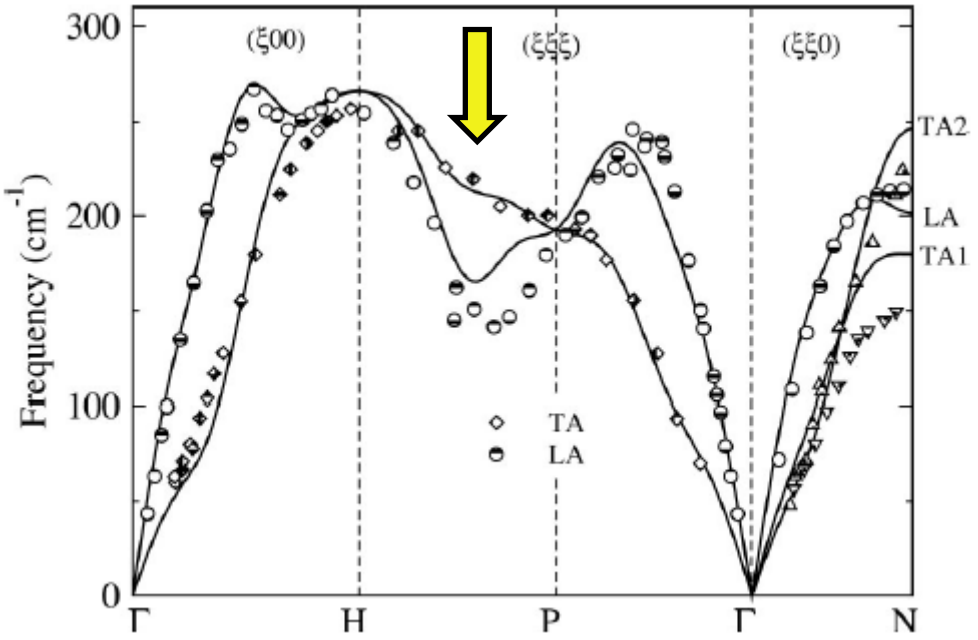

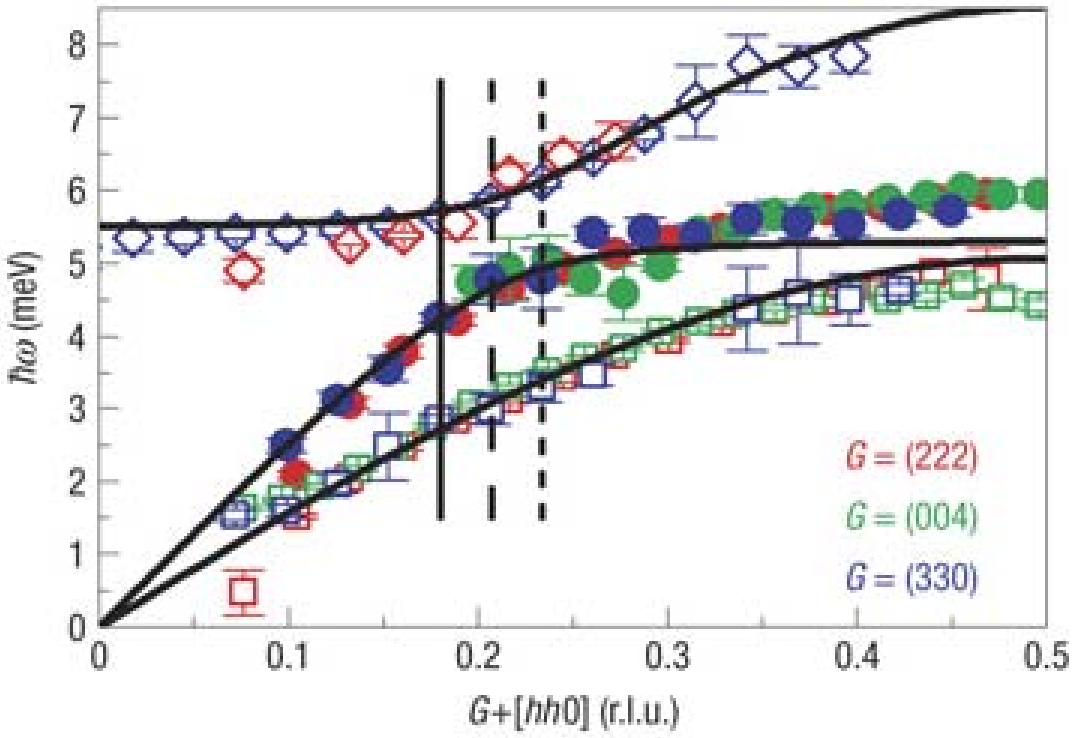

$Ba_8Ga_{16}Ge_{30}$

optical-acoustic coupling (anticrossings)

$BaTiO_3$

perovskite

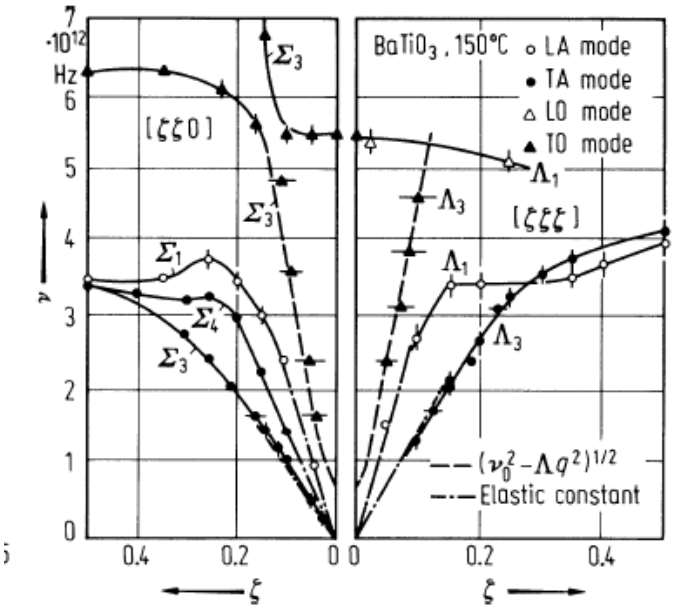

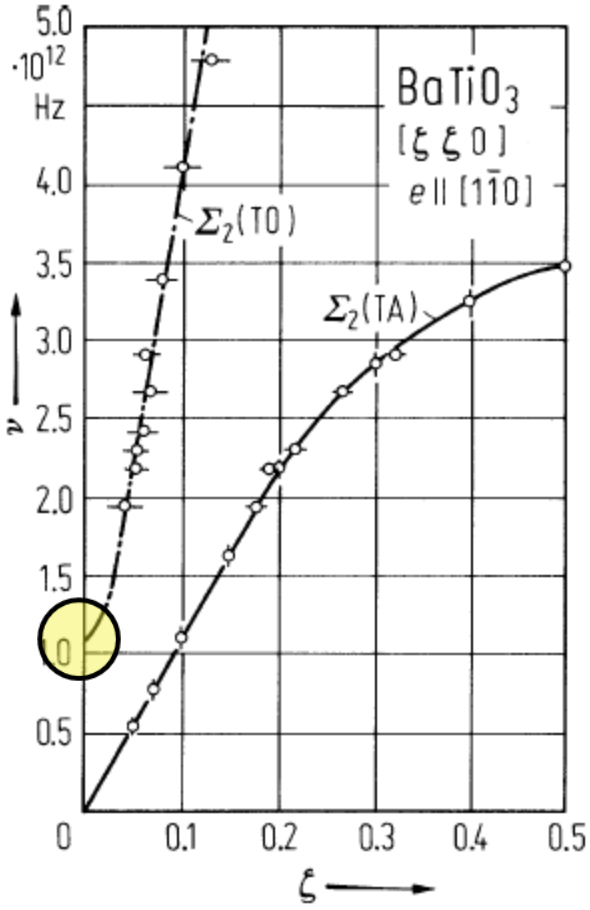

soft modes:
phase transitions

$(K_xRb_{1-x})_2SeO_4$

Soft Optical Modes, Phase Transitions and Internal Modes (molecular crystal)

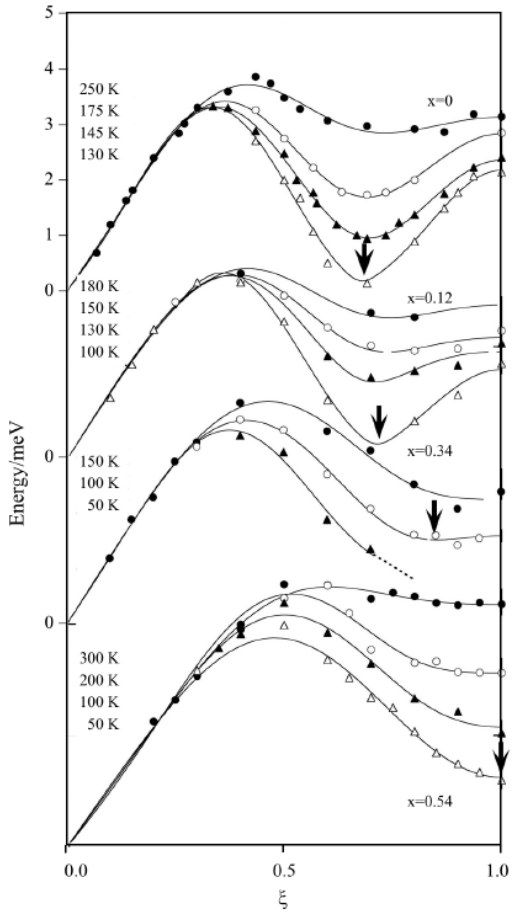

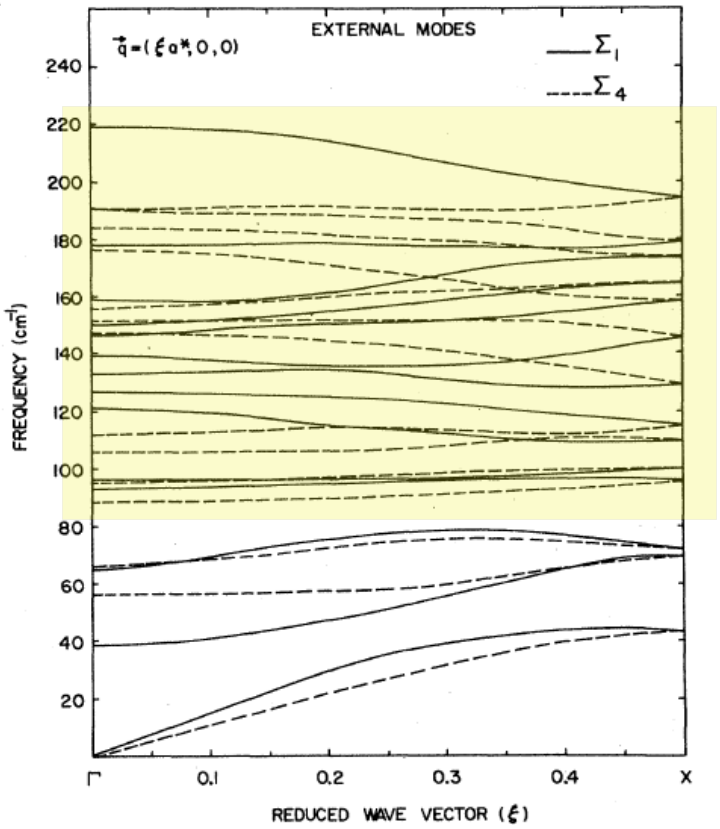

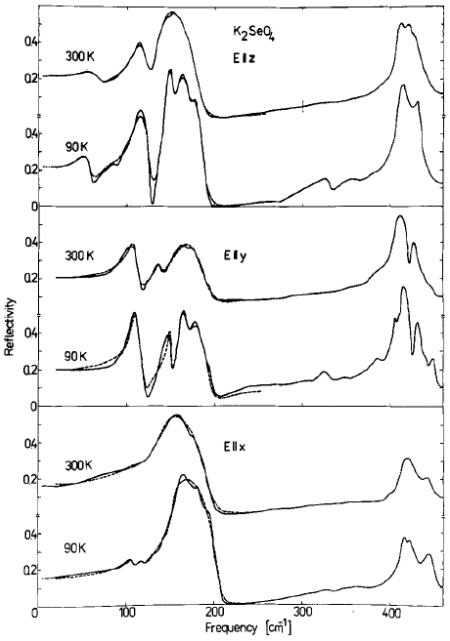

Infrared Reflectivity

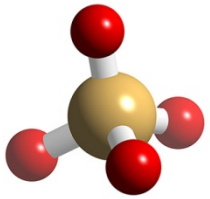

SeO_4

molecular crystal:
Anthracene

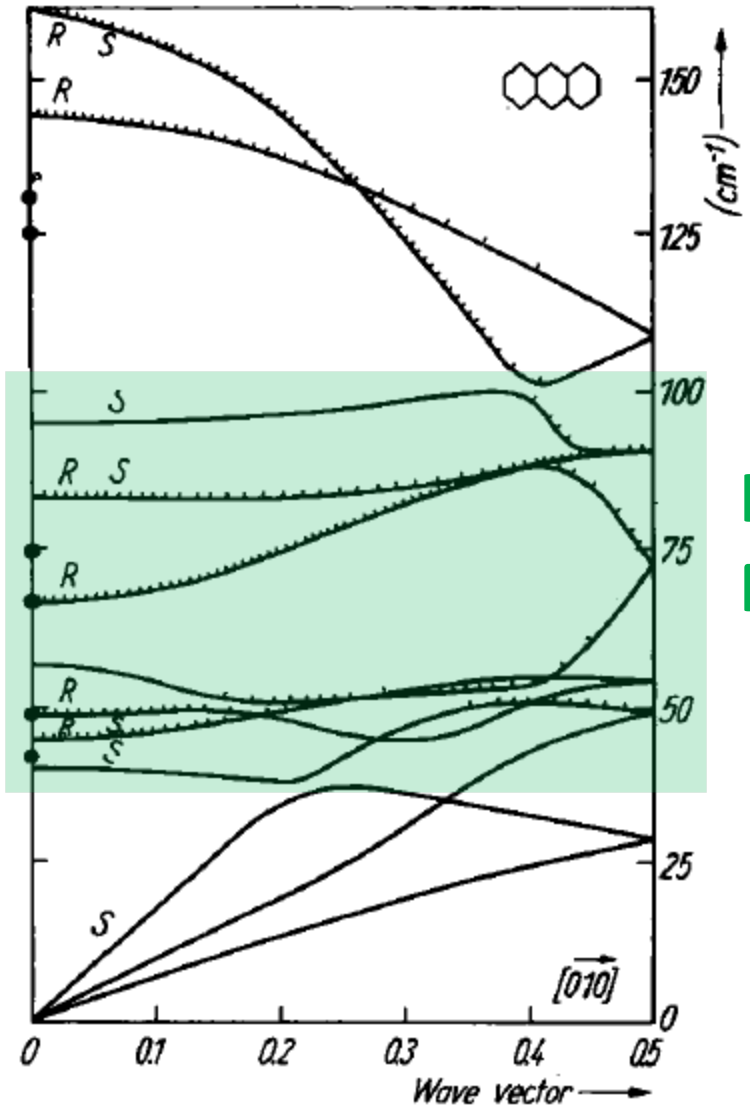

Internal Modes

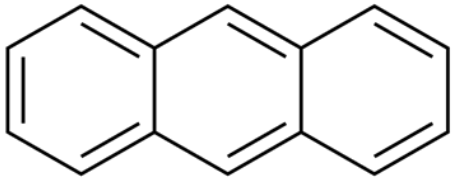

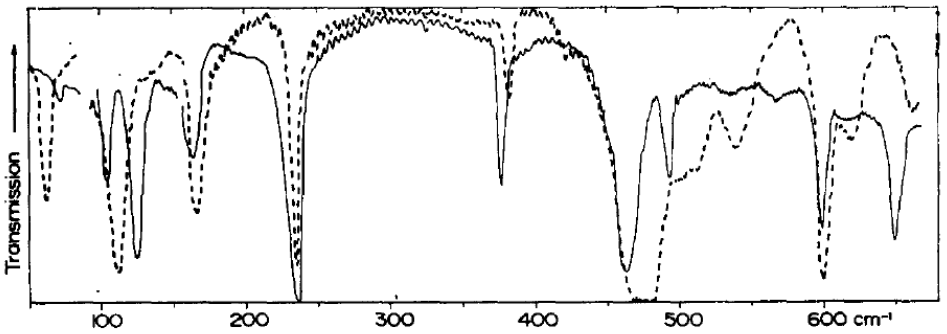

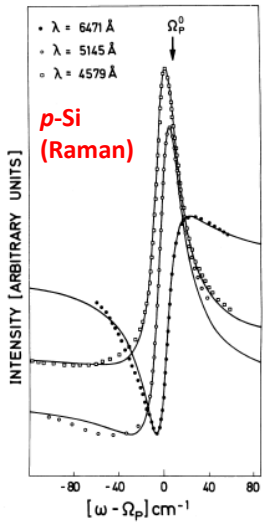

FIG. 2. Portion of the spectrum corresponding to scattering by zone-center phonons for different scattering wavelengths. The solid lines are theoretical fits with Eq. (12) to the experimental curves (discrete points). Ω_P^0 and Ω_P denote the zone-center phonon frequency of the intrinsic and doped materials, respectively.

Phys. Rev. B **9**, 4344

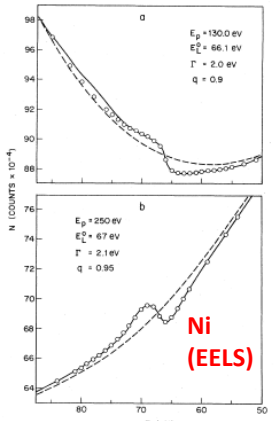

FIG. 1. Plots of the electron energy-loss distribution for Ni(001) in the vicinity of the 3p excitation for two different values of the primary energy E_p. The full lines are experimental $N(E_L)$ curves. The circles indicate values calculated from Eq. (1). The background curves $N_0(E)$ (broken lines) and the values assigned to M^2 in Eq. (1) were (a) $N_0(E) = 285.21 - 46.593E^{1/2} + 2.7566E$, $M^2 = 0.9$; (b) $N_0(E) = 954.50 - 142.42E^{1/2} + 5.691E$, $M^2 = 1.3$. The background parameters were generated by assuming that the contribution of the resonance to the background was negligible at points 25 eV on either side of E_L^3. The value of the background at E_L^3 was then taken as a parameter and adjusted along with Γ and q so as to give a best fit. Using this procedure a unique fit could be obtained for the parameters to within the uncertainties quoted in the text.

Phys. Rev. Lett. **33**, 1372

Rb vapor (EIT)

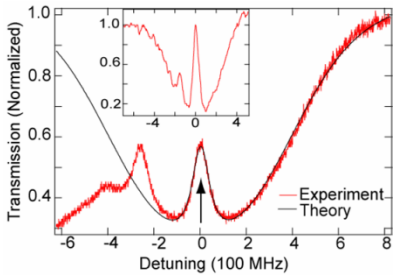

Phys. Rev. Lett. **97**, 023603

WG Modes

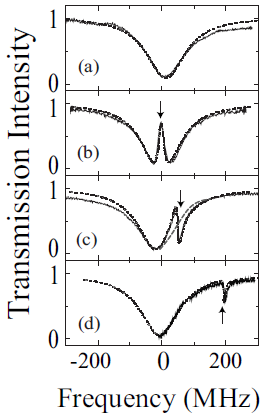

Fig. 2. Solid curves and dashed curves are experimental and theoretical spectra in the coupled microsphere resonators under the following conditions: (b) $\nu_1 \simeq \nu_2$, (c) $\nu_1 < \nu_2$, $\Delta\nu_{12} = \nu_2 - \nu_1 < \delta\nu_1$, and (d) $\nu_1 < \nu_2$, $\Delta\nu_{12} > \delta\nu_1$. Arrows indicate the resonance frequency of the second sphere, ν_2. The detuning parameter is (b) $\Delta\nu_{12} = 0$ MHz, (c) $\Delta\nu_{12} = 49$ MHz, and (d) $\Delta\nu_{12} = 204$ MHz. Other parameters used in the calculations are $x_1 = 0.999{,}432$, $x_2 = 0.999{,}973$, and $y_1 = 0.999{,}651$ in all figures. The coupling parameter between two spheres is $y_2 = 1$ in 2(a), while $y_2 = 0.999{,}999{,}960$ in 2(b)–2(d). The gray dashed line in 2(c) is the transmission dip by the naked first sphere as a reference. (a) is the spectrum observed without S_2.

JOSA B **26**, 813

Fano Interferences

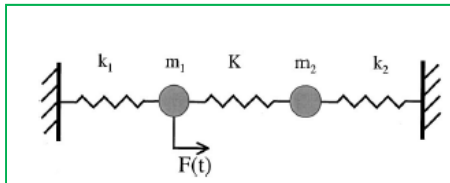

Fig. 2. The mechanical model used to simulate EIT.

Am. J. Phys., Vol. 70, No. 1, January 2002

Phys. Rev. **135**, A1732 (1964)

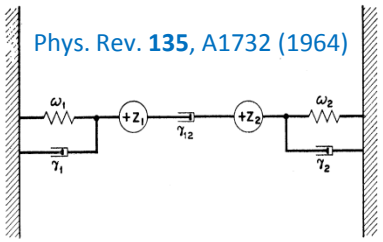

FIG. 2. Mechanical model of two optic mode oscillators with interaction damping. The dashpots γ_1, γ_2, and γ_{12} provide damping forces proportional to velocity.

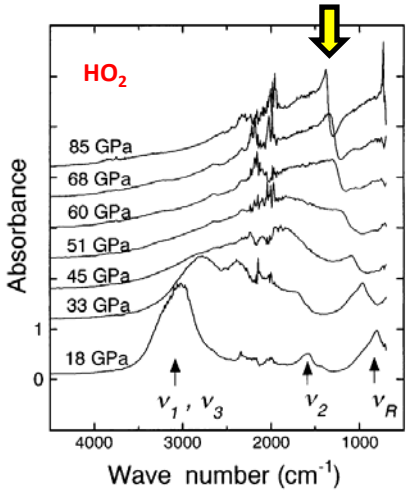

Phys. Rev. Lett. **76**, 784

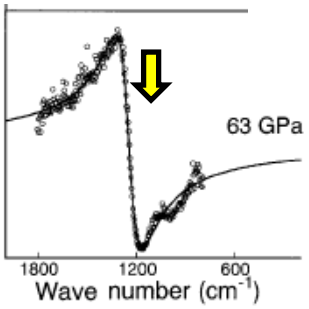

Coupled Modes:
Interference-Induced Transparency

DIRECT WANNIER EXCITONS

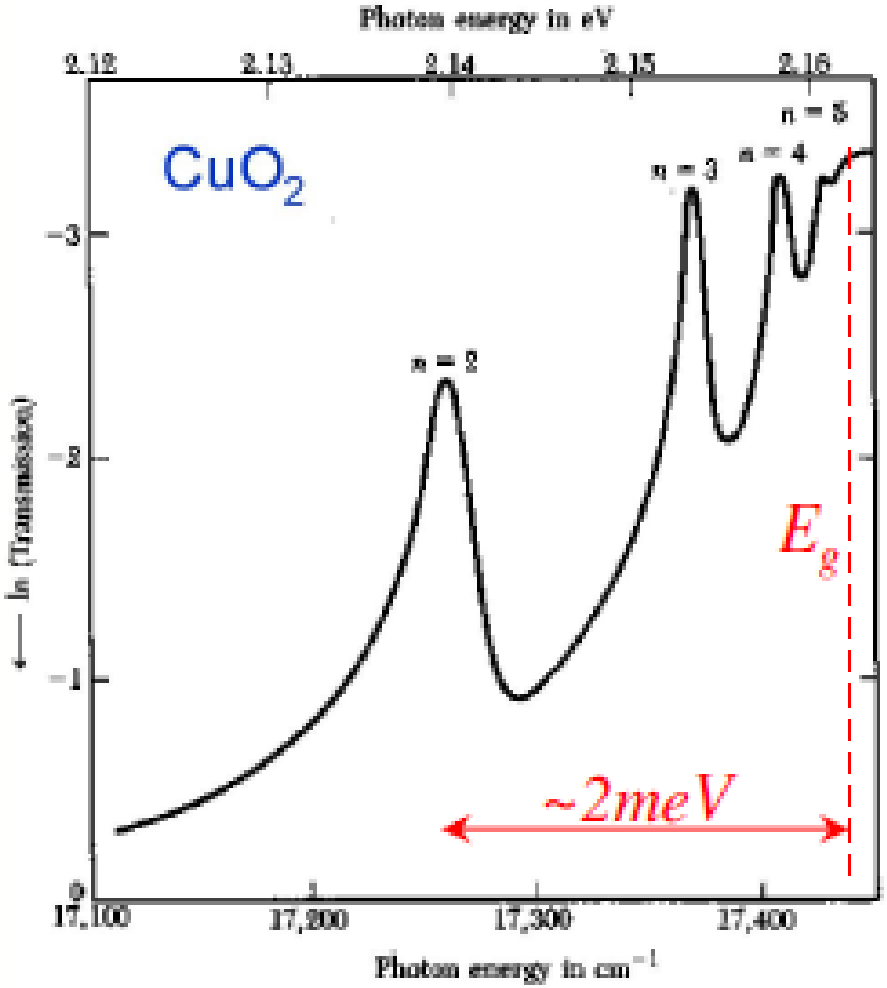

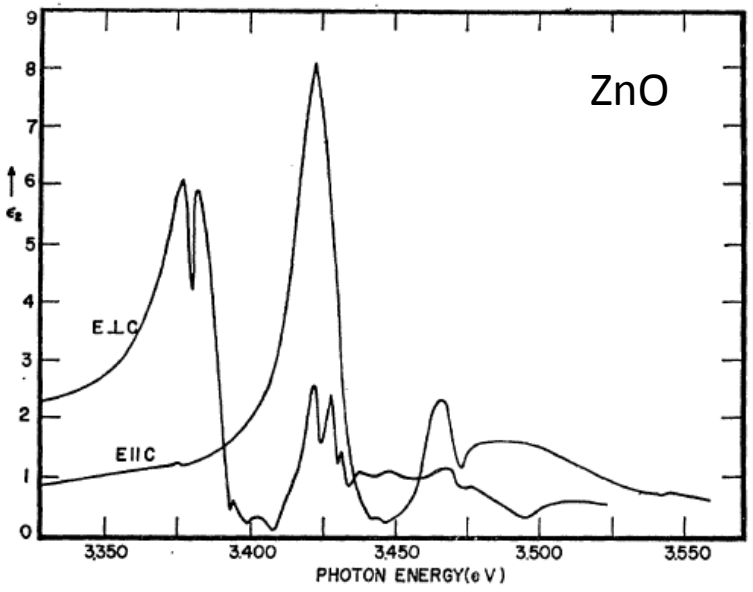

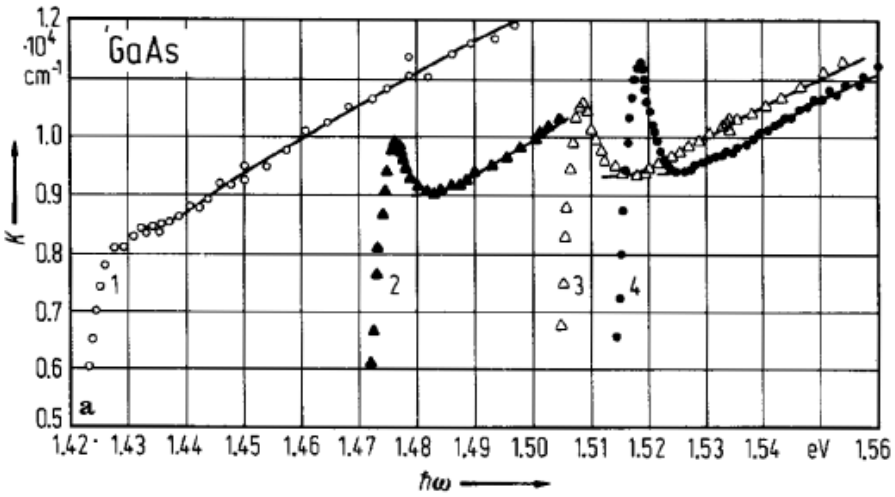

FRENKEL EXCITONS

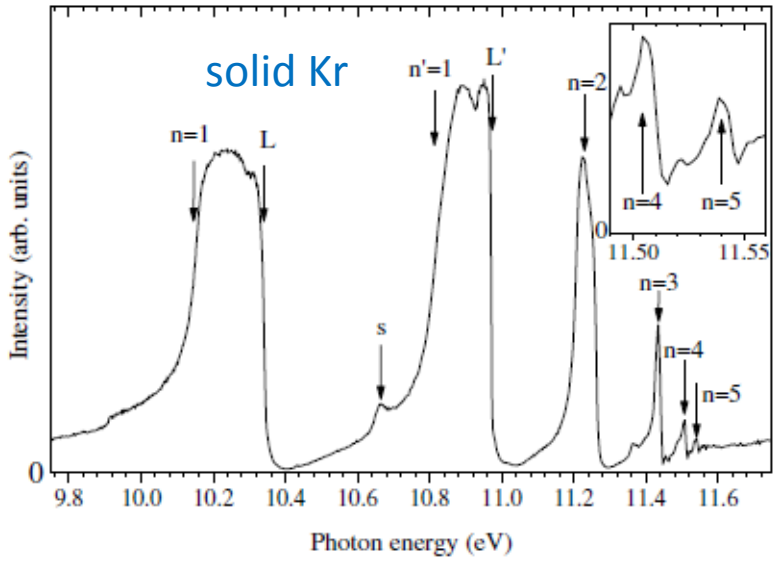

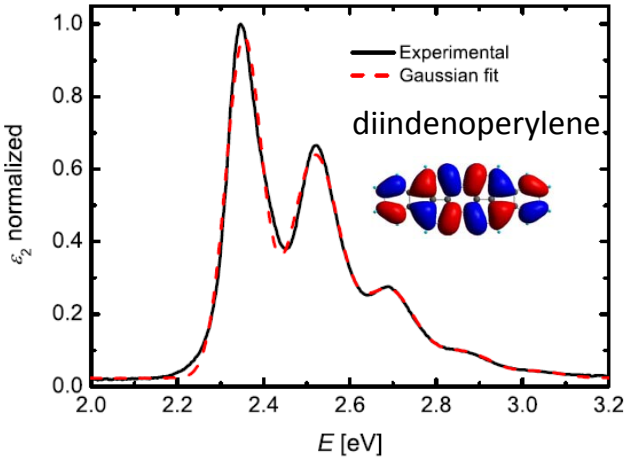

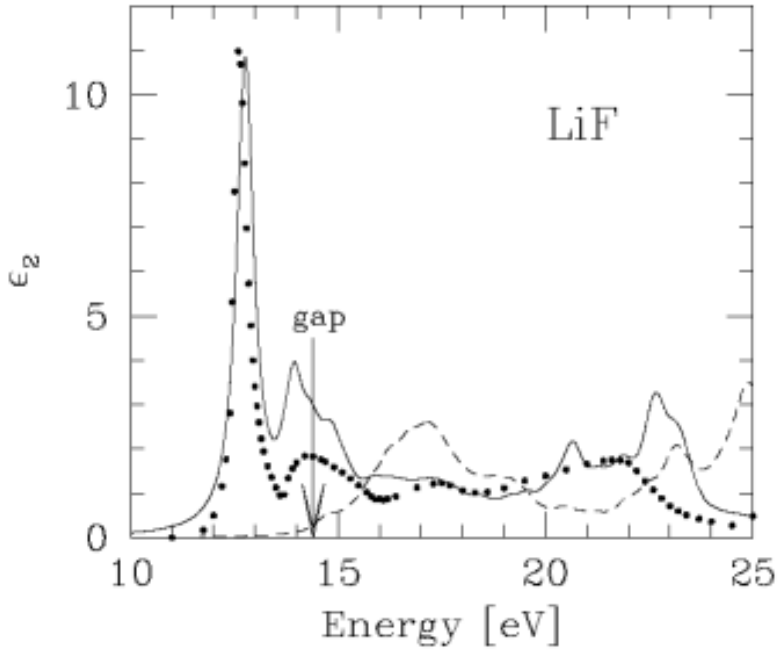

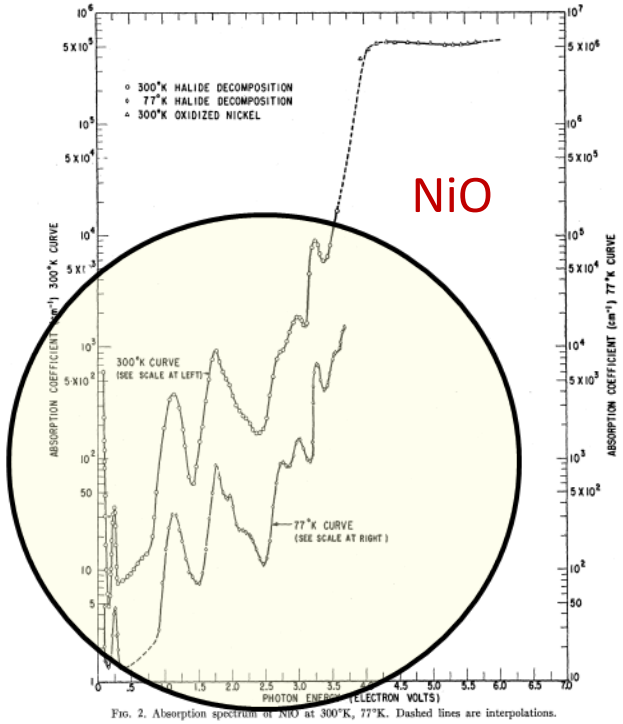

magnetic-dipole

INDIRECT WANNIER EXCITONS

Germanium

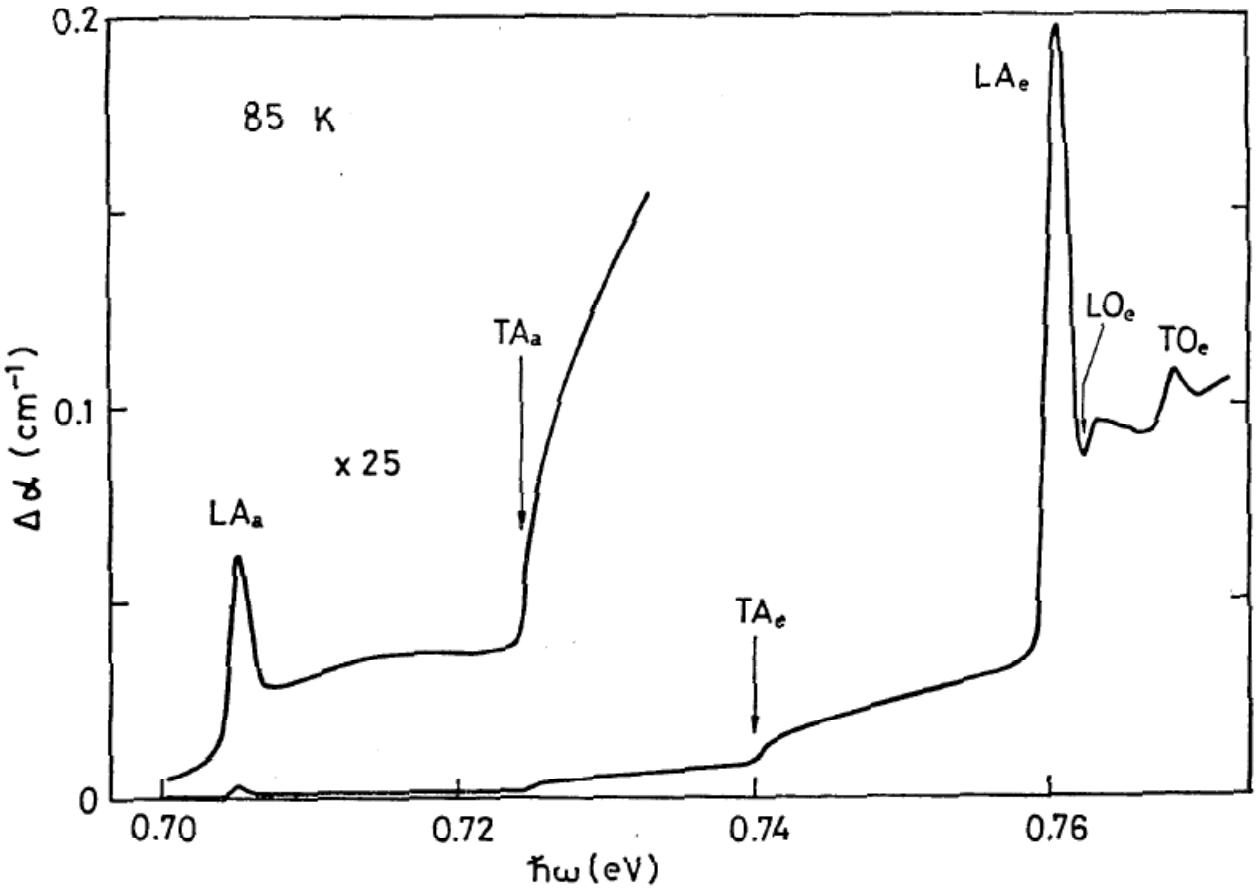

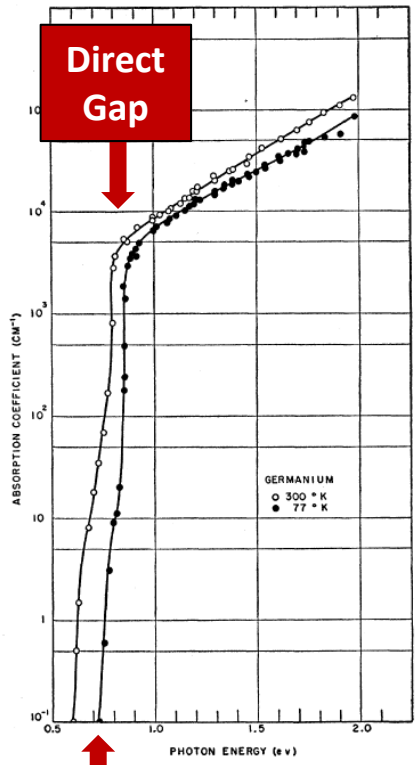

J. Phys. Soc. Japan **37**, 1016 (1974)

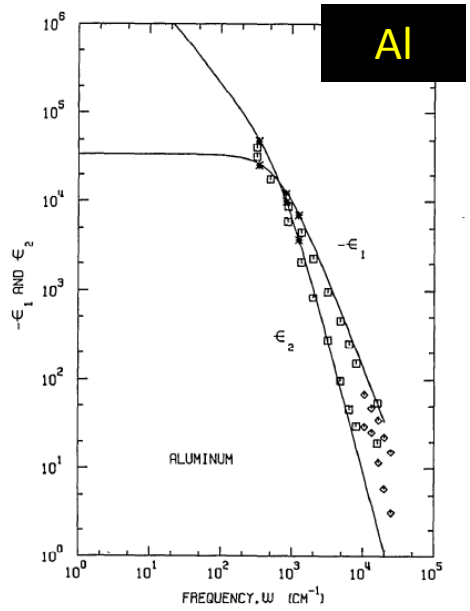

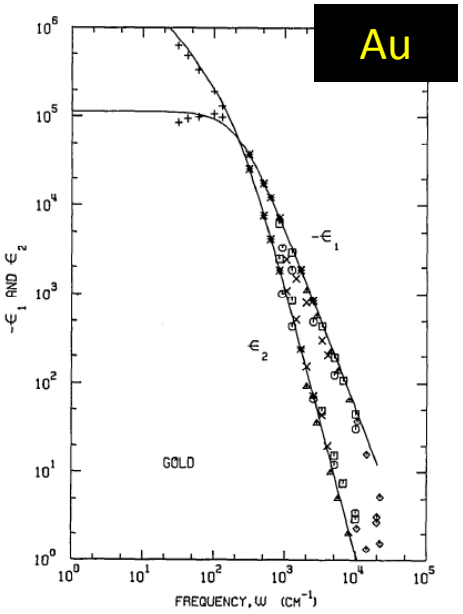

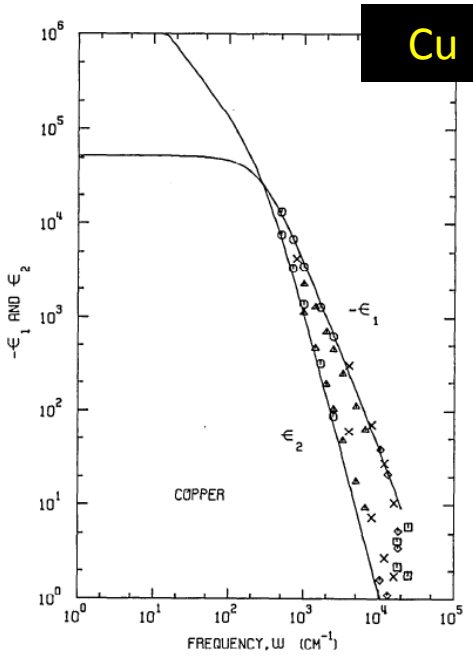

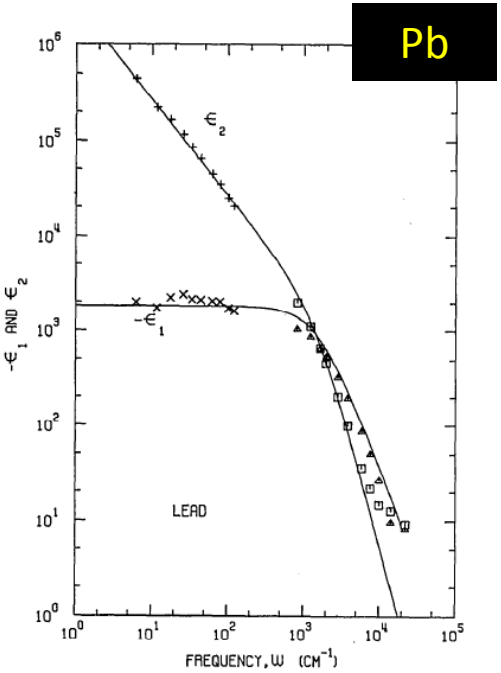

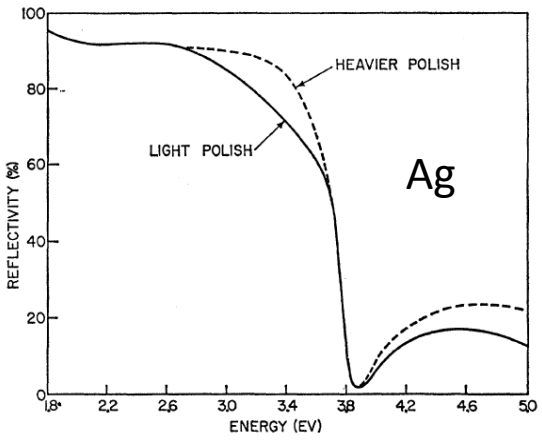

interband transitions

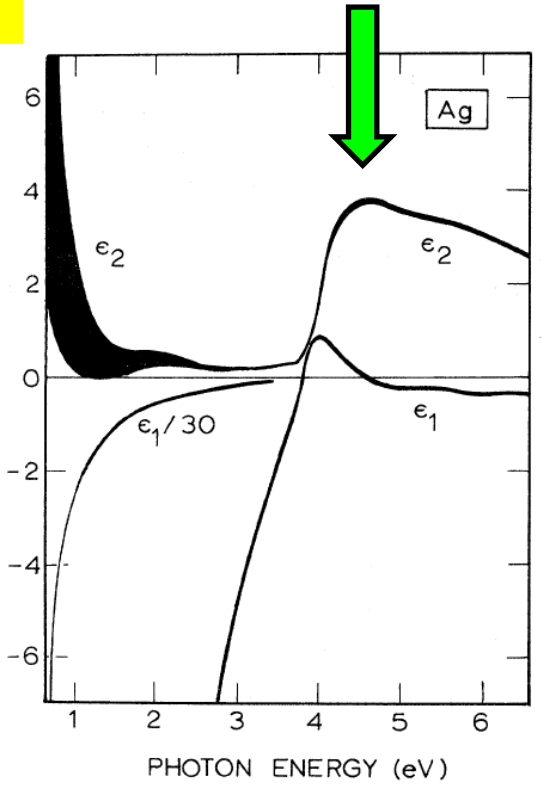

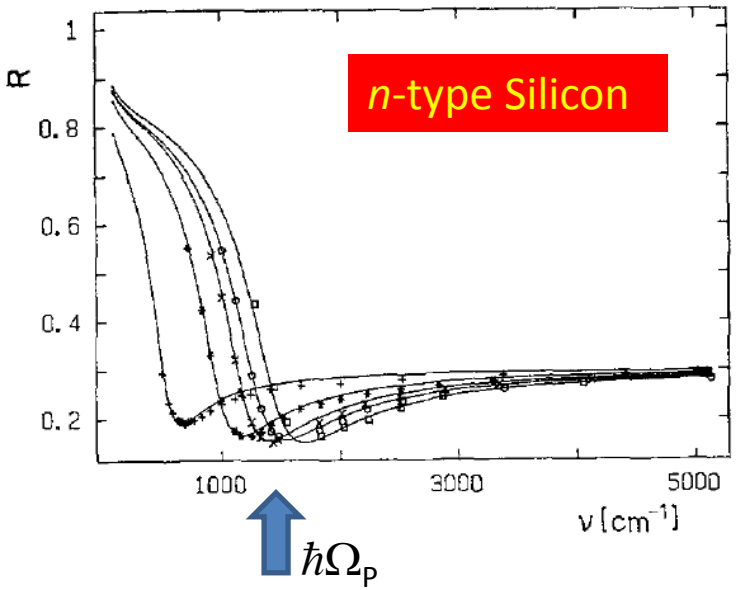

n-type Silicon

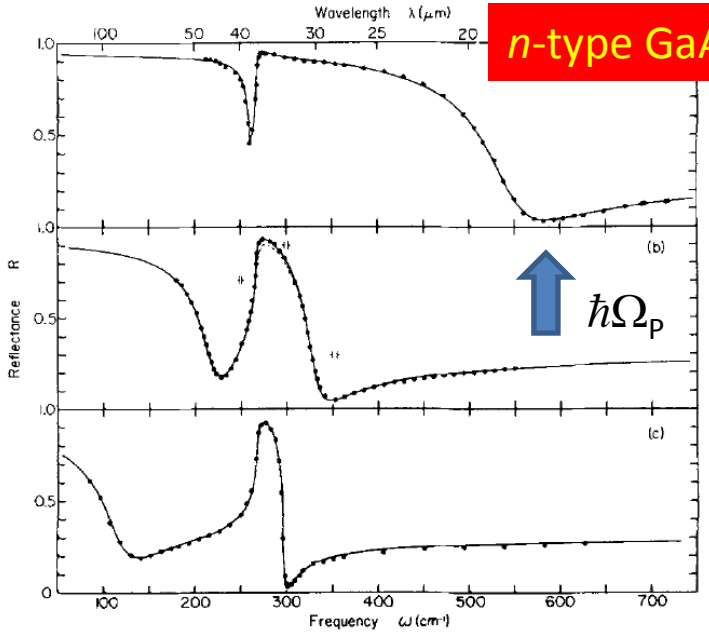

n-type GaAs

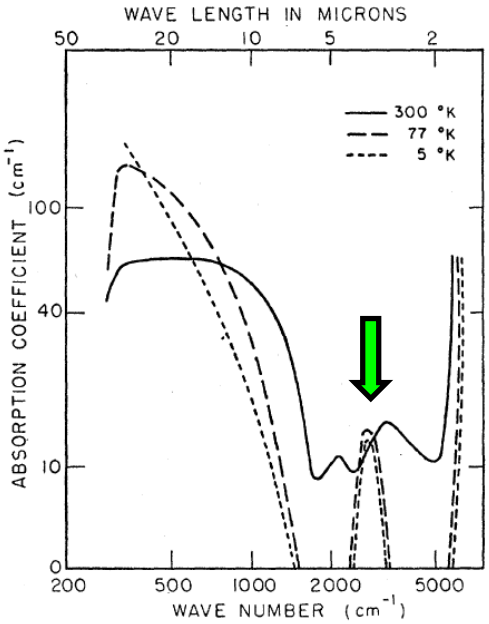

experiment

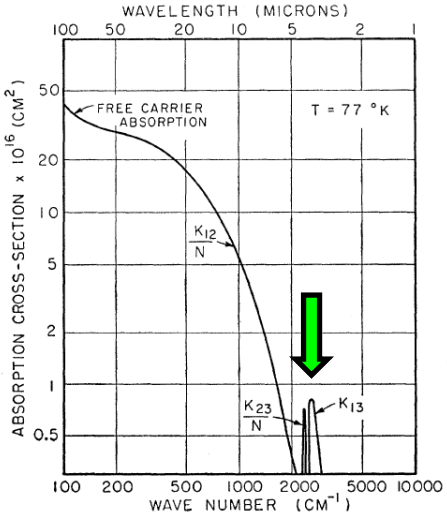

theory

interband transitions

valence band

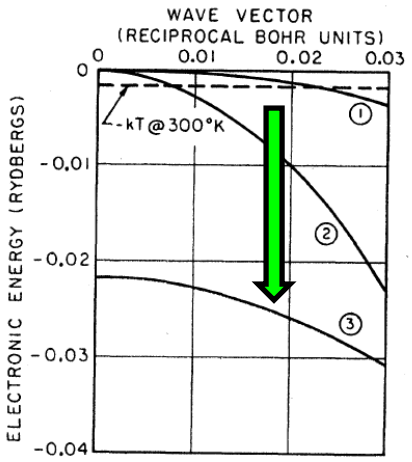

p-type Ge